CC Technologies
SOLVING MATERIALS PROBLEMS
THROUGH INNOVATION

September 8, 1998

Mr. Clare A. Paul
AFRL/VASE
Bldg. 65, 2790 D Street, Rm. 504
Wright-Patterson AFB OH 45433-7402

Re: Draft Final Report, Contract No. F33615-97-C-3215

Dear Clare:

Enclosed is a draft copy of our Final Report of the above referenced STTR project, entitled "Mathematical Model to Predict Fatigue Crack Initiation in Corroded Lap Joints". We enjoyed working on this project and are looking forward to the opportunity to continue to work on this important topic.

Sincerely,

CC TECHNOLOGIES LABORATORIES, INC.

Gerhardus H. Koch, Ph.D.
Vice President

Enclosure

Senior Staff

Neil G. Thompson, PhD
President

John A. Beavers, PhD
Vice-President, Research

Kevin C. Garrity, PE
Vice-President, Engineering

Gerhardus H. Koch, PhD
Vice-President, Systems

Carl E. Jaske, PhD, PE
Senior Group Leader

Arun K. Agrawal, PhD
Senior Scientist

Philip D. Simon, PE
Senior Engineer

Thomas J. Barlo, PhD
Senior Group Leader

6141 Avery Road ■ *Dublin OH 43016-8761 USA* ■ 614.761.1214 ■ *fax 614.761.163*

MATHEMATICAL MODEL TO PREDICT FATIGUE CRACK INITIATION IN CORRODED LAP JOINTS

DRAFT

DRAFT

TECHNICAL REPORT

GERHARDUS H. KOCH

CC TECHNOLOGIES LABORATORIES, INC.

DUBLIN, OH 43016

LE YU AND NORIKO KATSUBE

THE OHIO STATE UNIVERSITY

COLUMBUS, OH 43210

AUGUST 1998

REPORT FOR PERIOD AUGUST 1997 – AUGUST 1998

APPROVED FOR PUBLIC RELEASE; DISTRIBUTION UNLIMITED

19990504 037

AFRL/VASE

WRIGHT PATTERSON AFB, OH 45433

DTIC QUALITY INSPECTED 4

FOREWORD

This report present the results of experimental and modeling studies to examine and simulate the effects of corrosion on the contact or faying surfaces of lap joints on the stress and strain distribution in the lap joint. The work was performed by CC Technologies Laboratories, Inc. and the Department of Aerospace Engineering, Applied Mechanics, and Aviation of The Ohio State University for the Air Force Research Laboratory (AFRL/VASE) under STTR Phase I Contract No. F33615-97-C-3215. The period of performance was from August 1997 through August 1998. Mr. Clare A. Paul (AFRL/VASE) was the Air Force Project Monitor.

EXECUTIVE SUMMARY

Many commercial and military aircraft have reached or exceeded their original design life, and have been subject to significant increases in maintenance and repair cost due to corrosion. While corrosion is now being recognized to having a detrimental effect on the structural integrity of aging aircraft components, the lack of predictive capability has prevented the operators of aging aircraft from successfully controlling corrosion.

Specifically, there is increasing concern about the potential detrimental effects of corrosion on the structural integrity of fuselage lap joints. This corrosion can lead to a decrease in strength as a result of loss in skin thickness, early fatigue crack initiation caused by the formation of stress risers, and increased fatigue crack growth rates. The mode of corrosion in lap joints has generally been considered to be uniform loss of material by crevice and exfoliation corrosion. In fact, the effect of corrosion on fatigue crack initiation and propagation in lap joints has been largely ignored, because present non-destructive inspection techniques are considered sufficient to detect corrosion before it affects the structural integrity of the joint.

In order to get a better handle on the effects of corrosion on the structural integrity of fuselage lap joints, CC Technologies Laboratories and The Ohio State University were

awarded a Phase I STTR project. The objectives of this project were to characterize the corrosion in a fuselage lap joint, and to demonstrate the feasibility to develop a mathematical model that can be used to identify sites in corroded lap joints, where fatigue cracking is likely to initiate. In order to meet these objectives, the research was divided into three separate tasks:

Task 1: Microscopic Characterization of Lap Joint Corrosion
Task 2: Finite Element Modeling of Lap Joint Corrosion
Task 3: Experimental Verification

The results of this research has clearly demonstrated that corrosion on the contact or faying surfaces of a fuselage lap joint can have a detrimental effect on the structural integrity of the joint. Contrary to the general assumption that corrosion in lap joints is uniform in nature, the metallographic studies described in this report, demonstrated that lap joint corrosion is complex and is a combination of various forms of corrosion. The most obvious is exfoliation corrosion, which is a special form of intergranular corrosion common in the 2024-T3 aluminum alloy. Initially, the grain boundaries are attacked and hydrated aluminum oxide, $Al_2O_3.3H_2O$, or aluminum hydroxide, $Al(OH)_3$ corrosion byproducts form at the grain boundaries. Since the volume of the corrosion byproducts is approximately six times that of the aluminum it replaces, the surface of the skin tends to swell. Once the exfoliated grains are surrounded by the corrosion byproduct, the grains will continue to corrode by preferential dissolution of aluminum, forming aluminum hydroxide. When these voluminous aluminum hydroxide corrosion byproducts form in the confined space between the two contacting skins of a lap joint, considerable pressure is exerted on to the skins. Since in the case of the KC-135 fuselage lap joint, the inside skin of the lap joint is supported by a longeron, the pressure inside the joint pushes out the outer skin. This results in bulging between the fasteners, also known as pillowing.

It was demonstrated in the literature, and confirmed in the present FEA work that the pillowing resulting from the build up of corrosion byproducts causes high stresses and

strains in regions adjacent to the fastener holes. These regions could well become preferential sites for fatigue crack initiation. Moreover, it was found by Komorowski et al. and Welch that once cracks form, they have semi-elliptical crack fronts with high aspect ratio's. These cracks will not break the surface and will therefore be difficult to detect. Also, it was pointed out by Welch that these cracks can propagate in directions other than perpendicular to the hoop stress, which can potentially lead to rapid loss of the lap joint function.

Detailed metallographic analysis of the lap joint section revealed that underneath the exfoliated grains regions of fine intergranular attack exist. These regions can be approximated by a hemisphere, which can deeply penetrate into the skin. Due to the tightness of the intergranular corrosion, it is very difficult to detect and recognize these regions of corrosion with the common NDI techniques, until they have completely penetrated the skin. The hemispheric envelopes of the intergranular corrosion were simulated with FEA in order to determine their effects on the stress and strain distribution of a pillowing skin between four fasteners. The results of the analyses indicate that the hemispheres increase the local stresses and strains, so that anyplace they form, they could act as nucleation site for fatigue cracking. Specifically, when hemispheres were placed at the location where the highest stresses and strain occurred as a result of pillowing alone, even small regions of intergranular attack would result in significant increases in stress and strain that fatigue cracking is likely to initiate.

Thus, based on the results presented in this report, it can be concluded that corrosion inside lap joints of aluminum alloy 2024-T3 is very complex. Some forms of corrosion observed are exfoliation corrosion, pitting, preferential dissolution, and intergranular corrosion. Due to the formation of voluminous corrosion byproducts inside the joint, the outer skin of the joint is pushed out, which results in high stresses around the fastener holes. The presence of local regions of intergranular corrosion under the exfoliated grains weakens the joint further by lowering the residual strength, and by creating sites for fatigue crack nucleation.

Based on this work, recommendations are made to further address the problem. First, the problem of detectability of exfoliation and intergranular corrosion must be addressed. As indicated before, it is extremely difficult to detect and recognize the corrosion in the lap joint, particularly the pockets of fine intergranular corrosion. Since little is known about the relationship between the different types of corrosion and non-destructive inspection (NDI) readings, it is recommended that correlations between NDI and lap joint corrosion be developed.

Secondly, once the extent and type of lap joint corrosion is known, its effect on the structural integrity of the lap joint must be determined. The current micro-level investigation of the effect of localized corrosion on the stress and strain distribution in fuselage lap joints needs to be further developed to include fatigue crack initiation and propagation. The finite element model predictions need to be verified experimentally with controlled localized corrosion, so that the initial stage of the fatigue life, which is fatigue crack initiation to through crack development, can be assessed. Since this stage of fatigue life is the longest and is possibly the most important, the proposed investigation and analysis combined with the measurement of pillowing displacement will provide a useful tool in determining the schedule for replacing fuselage panels.

In addition to the corrosion-fatigue interaction, the effect of localized corrosion on the residual strength of fuselage lap joints needs to be investigated. This effort will be rather difficult since the failure modes and criteria for residual strength on the local level are not well understood. In the macro-level study of through cracks, stress intensity factors are often used as measure of residual strength. However, the failure modes may be determined by the extent of the localized plastic region in corroded panels. Extensive experimental work with controlled corrosion morphology and fatigue cracks, coupled with the appropriate finite element models are needed.

TABLE OF CONTENTS

LIST OF FIGURES

1.0 INTRODUCTION

A large number of commercial and military aircraft have reached or exceeded their original design life, and they have been subject to a significant increase in maintenance and repair cost due to corrosion. Moreover, corrosion is now being recognized to have a major effect on the structural integrity of aging aircraft. The lack of predictive capability, however, has prevented the operators of these aircraft from successfully controlling corrosion in hidden or difficult-to-access areas.

Specifically, there is increasing concern about the potential detrimental effects of corrosion on the structural integrity of fuselage lap joints. Corrosion in these joints can lead to a decrease in strength as a result of thickness loss, early fatigue crack initiation caused by the formation of stress risers, and increased fatigue crack growth rates. The mode of corrosion in lap joints has generally been considered to be uniform loss of material by crevice and exfoliation corrosion, and no significance has been given to any localized form of attack such as pitting or intergranular corrosion. In fact, the effects of corrosion on fatigue crack initiation and propagation in lap joints have not been considered, because present non-destructive inspection techniques are considered sufficient to detect corrosion before it affects the structural integrity of the joint. Thus, present aircraft maintenance guidelines consider only thickness loss of the lap joint skin, which can affect the residual strength of the lap joint, and allow for a maximum loss in thickness of 10 percent within a single skin before repair must be made.

2.0 OBJECTIVE AND TECHNICAL SCOPE

The objectives of this project were to characterize the corrosion in a fuselage lap joint, and to demonstrate the feasibility to develop a mathematical model that can be used to identify sites in corroded fuselage lap joints, where fatigue cracking is likely to initiate. In order to meet these objectives, the research was divided into three separate tasks. These are:

Task 1: Microscopic Characterization of Lap Joint Corrosion.

Task 2: Finite Element Modeling of Lap Joint Corrosion.

Task 3: Experimental Verification

3.0 BACKGROUND

Over the past several years, much attention has been paid to the phenomenon of multi-site damage (MSD), particularly of fuselage lap joints. The concern about MSD of lap joints was triggered by the infamous incident on April 28, 1988 where an Aloha Airlines Boeing 737 flying at 24,000 ft (7,300 m) suffered a structural failure in which an 18 ft (5.5 m) section of the fuselage crown was torn. The aircraft landed safely, however, one life was lost.

An accident/failure investigation by the National Transport and Safety Board (NTSB) concluded that the failure had resulted from rapid and catastrophic crack growth caused by lap joint multiple site damage.[1] It is important to know that this particular aircraft had operated its entire life in a tropical marine environment. Thus, severe corrosion due to exposure to this environment could have eventually lead to MSD and catastrophic failure. At the very least, corrosion could have contributed to accelerated propagation of fatigue cracks. Extensive studies have been conducted to analyze and model MSD.[2-5] In these studies, MSD was generally considered to consist of small flaws, such as fatigue cracks originating from fastener holes, which could just be detected by standard NDI techniques. Generally, these cracks are greater than 0.05 inches. Again, environmental factors and corrosion have never played a significant role in MSD considerations. Although corrosion was considered to be a costly economic problem, it was not thought to affect the structural integrity of critical airframe structures, such as fuselage lap joints.[6]

Recently, much attention has been given to the phenomenon of pillowing of lap joints, where voluminous corrosion products at the contact or faying surfaces of a lap joint

cause deformation of the skin, see Figure 3.1. Work by Komorowski and coworkers[7-9] indicated that the volume increase associated with the corrosion products is approximately 6.5 times the volume of the corroded parent aluminum alloy. The large volume increase and resulting deformation of the skin likely results in high stresses near the fasteners, which can have a definite detrimental effect on the structural integrity of the lap joint by lowering the strength and providing preferential sites for fatigue crack initiation. Mathematical and finite element modeling by Komorowski[7-9] were used to simulate the presence of the voluminous corrosion products within the fuselage lap joint. The stresses in the skin, which result from the internal pressure by the corrosion product build-up, from the fasteners, and from the reduction in thickness caused by material loss were all taken into account. The results of the calculations indicated that the pillowing significantly increases the stress in a fuselage lap joint, particularly in the vicinity of the fastener holes.

Moreover, fracture mechanics analyses conducted by Bellinger and Komorowski[9], and Welch[10] revealed troubling cracking behavior in lap joints subject to pillowing. The analyses suggested that cracks would form on the faying surface, forming a semi-elliptical crack front with a high aspect ratio without breaking through the outer surface of the skin. This would make visual inspection of the crack difficult. Also, analyses by Welch suggested that these cracks would propagate in directions other than perpendicular to the hoop stress.

4.0 APPROACH

4.1 Task 1: Corrosion Characterization

While the above-discussed analyses were based on uniform loss of metal thickness as a result of crevice or exfoliation corrosion, no attempt was made to consider the actual lap joint corrosion morphology. It is reasonable to assume that localized corrosion,

such as pitting or intergranular corrosion, could have an adverse effect on the stress distribution in the lap joint, and further promote fatigue crack initiation and propagation.

In this task, a detailed characterization of the corrosion in a fuselage lap joint was performed using metallographic techniques. A section of corroded fuselage lap joint was removed from a KC-135 aircraft fuselage. This fuselage skin was made of aluminum alloy 2024-T3 sheet, and the original thickness of the lap joint section shown in Figure 4.1 is 40 mils (1 mm). After extensive visual inspection, areas for metallographic sectioning were selected. The selection of these areas was based on the appearance of corrosion both on the contact or faying surface and the outside surface. Generally, there was no evidence of corrosion on the outside surface of the skin, unless the corrosion had completely penetrated. The lap joint section was cut in different directions, longitudinally, transversely, and diagonally, so that the effect of orientation on the corrosion morphology could be examined, see Figure 4.2. The cut sections were mounted in epoxy, which was cured under vacuum. The metallographic cross sections were ground and polished with colloidal silica and magnesium oxide to 2 μm. In order to be able to study the corrosion morphology in three dimensions, several parallel and perpendicular cross sections were made.

In addition to the optical microscopic analyses, scanning electron microscopy (SEM) studies were performed on selected metallographic cross sections. Energy dispersive X-ray spectroscopy (EDS), which is a function of the SEM, was used to analyze the composition of specific corrosion by-products.

4.2 Task 2: Finite Element Analysis

Finite element analyses (FEA) were carried out using ABAQUS and I-DEAS. The I-DEAS program has the capability to automatically generate both two- and three-dimensional meshes, and is designed to interface with ABAQUS. In order to address the complex geometry of the type of corrosion in the fuselage lap joints, three different types of elements were tried to carry out the analyses. These elements were the 8-

node plane strain element, which is two-dimensional, the 20-node block element and the 10-node tetrahedron element. The latter two are three-dimensional elements. Based on preliminary results, it was decided to use 10-node quadratic tetrahedron elements. The mesh of tetrahedron elements was automatically generated by I-DEAS and imported to ABAQUS for finite element calculation and post-processing.

The finite element analysis was performed on a 1.0 square inch 0.04 inch thick sheet, which was reduced in thickness to 0.036 inches to simulate a 10 percent loss in thickness due to uniform corrosion attack. The distance between the four fastener holes in the coupon was 1 inch, and the dimensions of the holes were modeled after those of the fuselage lap joint section examined in this study, tapered holes with a 0.14 inner radius and 0.18 inch outer radius. A hemispherical pocket representing a region of localized corrosion was superimposed onto the uniformly corroded area. The material properties used for the finite element analyses were those for aluminum alloy 2024-T3 with the Young's modulus of 10,700 ksi and the Poisson's ratio of 0.33. Finally, linear elastic deformation was assumed in the analysis.

The stress and strain distribution on the lap joint section were calculated, based on a 1psi uniform hydrostatic pressure, which simulates the pressure produced by the corrosion by-product. Throughout the analysis, the symmetry condition was applied, so that one quarter of the boundary value problems could be analyzed. When necessary, the macro-micro analysis was used to improve the accuracy and efficiency of the model. Macro models based on a relatively coarse mesh were used first, and the calculated displacement fields were then used as boundary conditions for the fine-meshed micro models, which were used to represent the regions of localized corrosion.

4.3 Task 3: Experimental Verification

In this task, an experiment was designed to demonstrate the effect of pillowing and localized corrosion on the stress distribution on the surface of a 40 mil (1 mm) sheet of alloy 2024-T3. The test coupon was a 1.5 square inch alloy sheet with a 0.25 inch

diameter chamfered hole in each corner. The hole dimensions were the same as those in the lap joint (0.25 inch outer diameter with a 10 degree chamfer). The test fixture, which was designed to simulate the stresses induced by the build-up of corrosion products, consisted of a steel ball base over which a corroded alloy 2024-T3 sheet was pushed, see Figure 4.3. The posts were fastened to the chamfered holes of the test specimen to simulate fasteners.

As the ball was pushed into the test specimen using a servo-hydraulic machine (see Figure 4.4), the test specimen deformed in a manner similar to that of the corrosion product induced deformation in the lap joints. The cross head speed during the tests was 0.01 inch per minute. It should be noted that in the laboratory set up the sides of the test coupon were not constrained. During the test, the strain gauge readings were recorded as a function of the crosshead displacement and load.

The corrosion on the test coupons was introduced with standard techniques, i.e. a four-day exposure to the standard EXCO solution.[11] Localized corrosion sites were introduced by exposing masked coupons with small openings (0.1 x 0.1 inch) on one surface to the solution. During the deformation, the strain was measured with rosette strain gages, which were attached at different locations on the outside of the test coupon. Figures 4.5 and 4.6 show a photograph of a test coupon, and a schematic drawing with the corrosion sites and locations of the strain gages, respectively.

5.0 RESULTS

5.1 Task 1: Corrosion Characterization

As shown in Figure 5.1, the outside of the lap joint shows little or no evidence of corrosion, but on the contact or faying surface of the lap joint, voluminous corrosion products, which are characteristic of exfoliation corrosion, can be observed. For example, Figure 5.2 shows a section of the lap joint with copious amounts of white colored corrosion product, hydrated Al_2O_3 or $Al(OH)_3$, which is thought to be responsible for the pillowing effect and resulting stresses on the skin and fasteners.

Metallographic cross sections through the lap joint section, such as shown in Figures 5.3 and 5.4, show extensive corrosion of the aluminum alloy skin, including pitting, exfoliation corrosion and intergranular corrosion. The figures show that exfoliation corrosion can either start from the faying surface or from a fastener hole. In the latter case, exfoliation can propagate over long distances before sufficient corrosion product is build up to create the pillowing effect. Once sufficient corrosion product has formed, lifting of the grains is observed, which is characteristic for severe exfoliation corrosion. Once the grains are lifted off, and surrounded by the hydrated aluminum hydroxide, corrosion of the alloy grains continues by an apparent form of dealloying corrosion. The optical micrographs of exfoliated grains, shown in Figure 5.5, clearly demonstrate the dissolution process of the grains. Specifically, the micrographs show remnants of the corroded grains indicating a selective dissolution process. In order to gain further insight into this particular mode of corrosion, a metallographic cross section was examined with energy dispersive X-ray spectrography (EDS) in a scanning electron microscope (SEM). The scanning electron micrographs in Figure 5.6 show a exfoliated grains with one grain showing evidence of dealloying corrosion. The EDS analysis of the exfoliated grain in Figure 5.7 indicates that the grain was depleted aluminum. Some copper and manganese rich areas and particles remained as indicated by the EDS spectrographs.

Further examination of several metallographic cross sections through the lap joint section demonstrated the presence of localized regions of intergranular corrosion in the aluminum alloy skin under the exfoliated regions. A series of optical micrographs in Figures 5.8 to 5.13 show intergranular attack to occur along grain boundaries and subgrain boundaries. This intergranular attack is very tight, which suggests that the voluminous aluminum hydroxide corrosion byproducts had not yet formed. Perpendicular cross sections such as shown in Figure 5.10 suggests that these regions of intergranular attack occur in the form of approximate hemispheres, and can propagate deep into the skin. In some case, it was found that the intergranular attack had occurred along a single path, which is characteristic of intergranular stress-corrosion cracking. Finally, there is evidence that that the voluminous aluminum hydroxides will eventually form along the grain boundaries, which will lead to exfoliation corrosion, see Figure 5.13.

5.2 Task 2: Finite Element Modeling

5.2.1 Benchmark Analyses

A square plate with dimensions of 1 inch x 1 inch x 0.036 inch, with pinned corners, and subjected to a uniform 1psi pressure was used for benchmark calculations. Initially, it was attempted to create a two-dimensional model. The cross sections through the plate were rectangular, and assuming that plane strain conditions existed on these cross sections, 8-node plane strain elements were used to calculate the displacement of the plate. The vertical displacement distributions for various cross sections were compared with those calculated from Timoshenko's plate theory. The fact that there was a 50% discrepancy between displacement results from the two-dimensional model and Timoshenko's plate theory indicated that the plane strain assumption was incorrect. Thus, the two-dimensional model approach was abandoned, and three-dimensional models were used.

Twenty-node block and 10-node tetrahedron elements were used to examine the effect of pillowing on the stress and strain distribution of a square plate of 1 inch x 1 inch x 0.036 inch, with pinned corners and subjected to a uniform 1 psi pressure. Because of symmetry considerations, one quarter of the plate was analyzed, as shown in Figure 5.14. The vertical displacement distribution was again calculated, and compared with the plate theory by Timoshenko, as shown in Figure 5.15. The analyses with block elements and tetrahedron elements yielded the same results. Two plate thicknesses of 0.036 inch and 0.018 inch were used, which required 8880 and 5719 10-node tetrahedron elements, respectively. The results of this comparison indicated that there is an approximately 5% difference between the three-dimensional FEA results and the theoretical results when a plate thickness of 0.036 inch is used. When the plate thickness is reduced to 0.018 inch, the FEA and theoretical results match. Since the theoretical results are based on the thin plate assumption, the FEA results are considered reasonable. The 5% error for the case of the 0.036-inch thick plate comes from the difference between the three-dimensional numerical analysis and the two-dimensional approximate analytical analysis.

5.2.2 Pinned Plate with Localized Fields of Corrosion

Following the FEA of a pinned plate subject to uniform metal loss and pressure due to corrosion by-products, pillowing joints with fields of localized corrosion were investigated. A hemisphere with a radius of 0.018 inch was superimposed on the uniform corrosion at different locations of the plate to simulate a hemispheric envelope around a localized region with intergranular corrosion. The initial location was at the middle of the plate. The stress-strain fields were calculated on one quarter of the plate using the 10-node tetrahedron elements. Since the hemisphere was very small compared to the size of the plate, a very fine mesh was needed in the region of the hemisphere, so that accurate results could be obtained. However, in the region away from the hemisphere, a coarse mesh could provide adequate precision. In order to obtain optimal results and to improve the efficiency of the calculations, macro-micro models were created, as shown in Figure 5.16.

For the macro model, a coarse mesh of 6189 10-node tetrahedron elements was used. This macro model had only one element in the thickness direction, but provided good displacement results over the entire plate, except at the small hemisphere. Thus, a micro model of 15,606 finer 10-node tetrahedron elements was created at the hemisphere site, covering a 0.1-inch radius area. The displacement field obtained from the FEA of the macro model was used to determine the boundary conditions, for the boundary value problem of the micro model at the hemisphere. The specified uniform pressure boundary conditions were shown to be satisfied along the hemispherical surface with less than a 5% error. Also, the number of elements of the micro model was doubled in order to generate an even finer mesh. The same boundary problems were solved for this micro model, and comparison of the two micro models indicated that the first micro model was sufficiently accurate.

The results of the micro model demonstrated a significant increase in strain at the hemisphere, as shown in Figure 5.17. While without the presence of the hemisphere in the plate, the normal strain in the diagonal direction was 0.0135, the presence of the hemisphere increased the local strain by 30% to 0.016. However, the maximum displacements perpendicular to the plate surface (z-direction) were the same at 0.129 inch for both cases.

In order to examine the effect of localized corrosion closer to the pin connection, the small hemisphere (0.018-inch radius) was positioned on the diagonal of the plate 0.05 inches from the pin, as in Figure 5.18. Symmetry conditions required that four hemispheres be located on the plate. As in the former case, one quarter of the plate was examined, using 1515 10-node tetrahedron elements for the macro model, and 14492 10-node tetrahedron elements for the micro model.

The results of the FEA indicated that the maximum strain occurred at the pin connection, which may overwhelm the effects of the superimposed hemisphere. Since the assumption of the pin connection itself is artificial, no quantitative value could be

given to the stress level at the pin. However, the maximum strain in the diagonal direction could be determined. This strain was 0.07, which is 89% higher than the strain of 0.037 in the absence of the small hemisphere, as shown in Figure 5.19.

5.2.3 Plate with Fastener Holes

The next step in the model development was to replace the pin connections with fastener holes. The dimensions of the fastener holes, with an inner radius of 0.14 inch and outer radius of 0.18 inch, were similar to those of the fastener holes in the in the fuselage lap joint described in sections 4.1 and 5.1. Again, because of the symmetry of the plate, one quarter of the plate was modeled using 3420 10-node tetrahedron elements. The displacement components of the fastener hole were assumed to be zero. When a uniform pressure of 1 psi was applied, the maximum normal strain in the diagonal direction of the plate was found to be 0.029 on the diagonal 0.198 inches from the center of the fastener hole, as shown in Figure 5.20.

In order to examine the effects of localized corrosion on the stress and strain distribution on the plate, a small hemisphere with a radius of 0.018 inches was placed on the diagonal 0.198 inches away from the center of the fastener hole. Figure 5.21 shows the mesh for the macro model with 14863 10-node tetrahedron elements. The local view of fine mesh around the hemisphere is shown in Figure 5.22. The location of the hemisphere was selected to coincide with the point where the normal strain in diagonal direction was the highest. With the 0.018-inch radius hemisphere, the maximum normal strain in diagonal direction is 0.0498, which occurs on the side where the hemisphere is located, see Figures 5.23 and 5.24. The strain at the location of the hemisphere is approximately 72% higher than the strain at the same location without the hemisphere. It is important to note that the calculations are based on the assumption of linear elasticity, and thus the magnitude of the maximum normal strain is well beyond the elastic range of the material.

After determining the effect of a 0.018-inch radius hemisphere on the stress-strain distribution near a fastener hole, the effect of size of the hemisphere was investigated. When the 0.018-inch radius hemisphere was reduced by a factor of two, as shown in Figure 5.25 (18998 10-node tetrahedron elements) and Figure 5.26, it was found that upon application of the 1-psi lateral pressure, the maximum normal strain was 0.053. This is illustrated in Figures 5.27 and 5.28. The strain for the smaller hemisphere is 6.6% larger than the strain calculated for the larger one. The results of these calculations indicate that the size of the hemisphere has a significant effect on the stress-strain distribution around the hemisphere, and that there is likely to be an optimal size at which the strain is at a maximum.

5.3 Task 3: Experimental Verification

The three-element rectangular rosette strain gages were placed at the 0, 45, and 90° positions, as indicated in Figure 4.5. From this rosette the cartesian components of strain ε_{xx}, ε_{yy}, and γ_{xy}, as well as the principal strains and stresses can be calculated.

The results of the strain measurements appeared to be only meaningful in those cases where the strain gages were attached to the middle of the test plate (see figure 4.6.) Upon loading, the steel ball made direct contact with the underside (contact or faying surface) of the plate, and thus the outside surface of the plate was loaded in tension. However , the material near the fastener holes was subject to a more complex loading mode of tension and compressive bending. Strain gages placed at these locations could therefore not accurately measure the stress state. In fact, the present experimental set up cold generally not reproduce the loading mode in an actual lap joint where uniform pressure is applied between four fastener holes, with the exception of the center of the plate. The rosette was placed such that one of the strain gages was oriented in the diagonal direction. Thus, the diagonal strain could be measured.

The test results of the plate with strain gages on the center of the plate indicate that corrosion has a severe effect on the local strain. Figure 5.29 shows the local strain at

the center of the plate in diagonal direction as a function of displacement for three different plate configurations. Number 1 represents the plate without corrosion; number 2 represents the plate with uniform corrosion of approximately 20 percent of the plate thickness; and number 3 represents the plate with a localized region of corrosion (0.1 x 0.1 inch) with approximately the same loss in thickness. For example, when taking a vertical displacement of approximately 0.06 inches, the results indicate that the local strain in diagonal direction changed from 0.00186 for the plate without corrosion to 0.00361 for the plate that is entirely corroded. When only a small region in the center of the plate was corroded with approximately the same thickness loss, the local strain increased significantly to 0.0129. These number are in approximate agreement with the FEA results for similar plate configurations.

6.0 DISCUSSION

The results of this research have clearly demonstrated that corrosion on the contact or faying surfaces of a fuselage lap joint could have a detrimental effect on the structural integrity of the joint. Contrary to the wide spread assumption that corrosion in lap joints is uniform in nature, the metallographic studies described in this report demonstrated that lap joint corrosion is complex and a combination of various forms of corrosion. The most obvious is exfoliation corrosion, which is a special form of intergranular corrosion common in the 2024-T3 aluminum alloy. Initially, the grain boundaries are attacked and hydrated aluminum oxide, $Al_2O_3.3H_2O$, or aluminum hydroxide, $Al(OH)_3$, corrosion byproducts form at the grain boundaries. Since the volume of the corrosion byproducts is approximately six times that of the aluminum it replaces, the surface of the skin tends to swell. Once the exfoliated grains are surrounded by the corrosion byproduct, the grains continue to corrode by preferential dissolution of aluminum, forming aluminum hydroxide. When these voluminous aluminum hydroxide corrosion byproducts form in the confined space between the two contacting skins of a lap joint, considerable pressure is exerted on to the skins. Since in the case of the KC-135 fuselage lap joint, the inside skin of the lap joint is supported by a longeron, the pressure inside the joint

pushes out the outer skin. This force results in bulging between the fasteners, also known as pillowing.

It was demonstrated in the literature, and confirmed in the present work that the pillowing resulting from the corrosion byproducts can cause high stresses and strains in areas adjacent to the fastener holes, which could then become preferential sites for fatigue crack initiation. Komorowski et al.[9] and Welch[10] described that cracks that formed at these sites have semi-elliptical crack fronts with high aspect ratio's, and will not break the surface. Therefore, these small cracks will be difficult to detect. It was further pointed out by Welch[10] that these semi elliptical cracks can propagate in directions other than perpendicular to the hoop stress, which could potentially lead to rapid loss of the lap joint function.

Detailed metallographic analysis of the lap joint section revealed regions of fine intergranular attack underneath the exfoliated grains. These regions can be approximated by hemispheres, which can deeply penetrate into the skin. Due to the tightness of the intergranular corrosion, it will be very difficult to detect and recognize these regions of corrosion with the common NDI techniques, until they have completely penetrated the skin. The hemispheric envelopes of the intergranular corrosion were simulated with FEA, so that their effects on the strain distribution of a pillowing skin could be calculated.

It was indicated before that the maximum strain on the plate as a result of uniform loss of plate thickness and pillowing is the highest near the fastener holes. When hemispheres are introduced at those locations of high strain, the resulting maximum strain increases significantly without affecting the vertical displacement of the plate. It was further found that the size of the hemisphere has a significant effect on the local maximum strain level. If the hemisphere is very small, its effect on the strain distribution is also small. If the hemisphere is relatively large (half the thickness of the plate), the localized effect is lost and the effect of uniform thinning and pillowing overwhelms the effect of the hemisphere. Thus, the localized high strain near the fastener hole depends

on both the pillowing and the formation of areas of localized corrosion, and preliminary calculations indicate that a hemisphere with a radius of a quarter plate thickness results in the highest local strain.

Thus, the results of the FEA indicated that the hemispheres would increase the local stresses and strains, so that anyplace they form, they could act as nucleation site for fatigue cracking. Specifically, when hemispheres were placed at the location where the highest stresses and strain occurred as a result of pillowing alone, even small regions of intergranular attack would result in significant increases in stress and strain that fatigue cracking is likely to initiate.

7.0 CONCLUSIONS AND RECOMMENDATIONS

Based on the results presented in this report, it can be concluded that corrosion inside lap joints of aluminum alloy 2024-T3 is very complex. Some forms of corrosion observed are exfoliation corrosion, pitting, preferential dissolution, and intergranular corrosion. Due to the formation of voluminous corrosion byproducts inside the joint, the outer skin of the joint is pushed out, which results in high stresses around the fastener holes. The presence of local regions of intergranular corrosion under the exfoliated grains weakens the joint further by lowering the residual strength, and by creating sites for fatigue crack nucleation. It was suggested by this work that a fatigue crack could initiate almost immediately when a localized region of corrosion of an appropriate size is introduced, and that the measurement of vertical or pillowing displacement alone is not sufficient to assess the structural integrity of fuselage lap joints. While the effects of corrosion on fatigue crack propagation has been examined, very little work has been done on the effect of specific corrosion morphologies on fatigue crack initiation and initial growth. The link between the micro-level knowledge of the state of localized corrosion and fatigue crack initiation, and existing macro-level knowledge of growth of through cracks is currently missing.

Recommendations can be made to further address the problem. First, the problem of detectability of exfoliation and intergranular corrosion must be addressed. As indicated before, it is extremely difficult to detect and recognize the corrosion in the lap joint, particularly the pockets of fine intergranular corrosion. Since little is known about the relationship between the different types of corrosion and non-destructive inspection (NDI) readings, it is recommended that correlations between NDI and lap joint corrosion be developed.

Secondly, once the extent and type of lap joint corrosion is known, its effect on the structural integrity of the lap joint must be determined. The current micro-level investigation of the effect of localized corrosion on the stress and strain distribution in fuselage lap joints needs to be further developed to include fatigue crack initiation and propagation. The finite element model predictions need to be verified experimentally with controlled localized corrosion, so that the initial stage of the fatigue life, which is fatigue crack initiation to through crack development, can be assessed. Since this stage of fatigue life is the longest and possibly the most important, the proposed investigation and analysis combined with the measurement of pillowing displacement will ultimately provide a useful tool in determining the schedule for replacing fuselage panels.

In addition to the corrosion-fatigue interaction, the effect of localized corrosion on the residual strength of fuselage lap joints needs to be investigated. This effort will be rather difficult since the failure modes and criteria for residual strength on the local level are not well understood. In the macro-level study of through cracks, the stress intensity factors are often used as measure of residual strength. However, the failure modes may be determined by the extent of the localized plastic region in corroded panels. Extensive experimental work with controlled corrosion morphology and fatigue cracks, coupled with the appropriate finite element models will be needed.

REFERENCES

1. "Aircraft Accident Report – Aloha Airlines, Flight 243, Boeing 737-200, N737111, near Maui, Hawaii, April 28, 1988", NTSB/AAR-89/03, National Transportation Safety Board Bureau of Accident Investigation, Washington, D.C., June 4, 1989.

2. Structural Integrity of Aging Airplanes, Eds. S. N. Atluri, S. G. Sampath, and P. Tong, Springer-Verlag, New York, 1990.

3. Durability of Metal Aircraft Structures, Proc. of International Workshop on Structural Integrity of Aging Airplanes, March 31-April 2, 1992 Atlanta, Eds, S. N. Atluri, C.E. Harris, A. Hoggard, N. J. Miller, and S. G. Sampath.

4. FAA/NASA International Symposium on Advanced Structural Methods for Airframe Durability and Damage Tolerance, Hampton, VA, May 4-6,1994, Ed. C.E. Harris.

5. FAA/NASA Sixth International Conference on the Continued Airworthines of Aircraft Structures, Atlantic City, NJ, June 27-28, 1995.

6. Lincoln, J.W. *The USAF Approach to Attaining Structural Integrity of Aging Aircraft,* Structural Integrity in Aging Aircraft, AD-Vol. 47, ASME 1995, pp. 9-19.

7. Bellinger N.C., S. Krishnakumar, and J. P. Komorowski, *Modelling of Pillowing Due to Corrosion in Fuselage Lap Joints,* Canadian Aeronautics and Space Journal, Vol. 40, No. 3, September 1994, pp. 125-130.

8. Bellinger, N.C., and J. P. Komorowski, and S. Krisnakumar, *Numerical Modelling of Pillowing Due to Corrosion in Fuselage Lap Joints,* LTR-ST-2005, National Research Council Canada, April 1995.

9. Bellinger, N. C., and J. P. Komorowski, *Implications of Corrosion Pillowing on the Structural Integrity of Fuselage Lap Joints,* Proceedings of the NASA-FAA Symposium on the Continues Airworthiness of Aircraft Structures, July 1997, pp. 391-401.

10. Welch, D. W., *Fracture Mechanics Analysis of a Corroded Aircraft Fuselage Lap Joint,* Master of Science Thesis, The University of Oklahoma, Norman OK, 1997.

11. ASTM G34-90, *Standard Test Method for Exfoliation Corrosion Susceptibility in 2XXX and 7XXX Series Aluminum Alloys (EXCO TESTS)*, American Society for Testing and Materials, 1990.

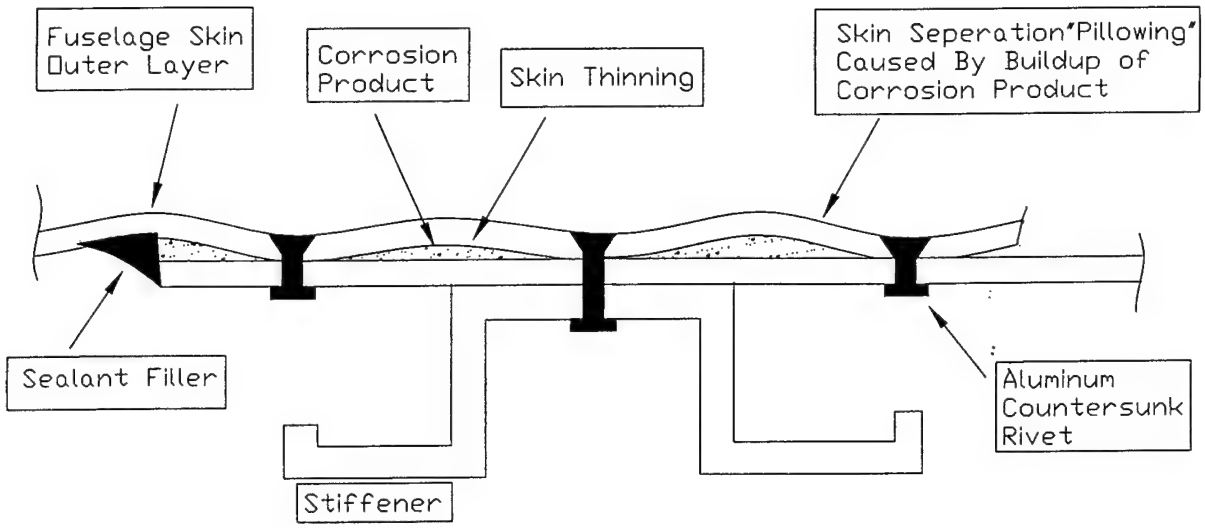

Figure 3.1. Cross Section Through Lap Joint.

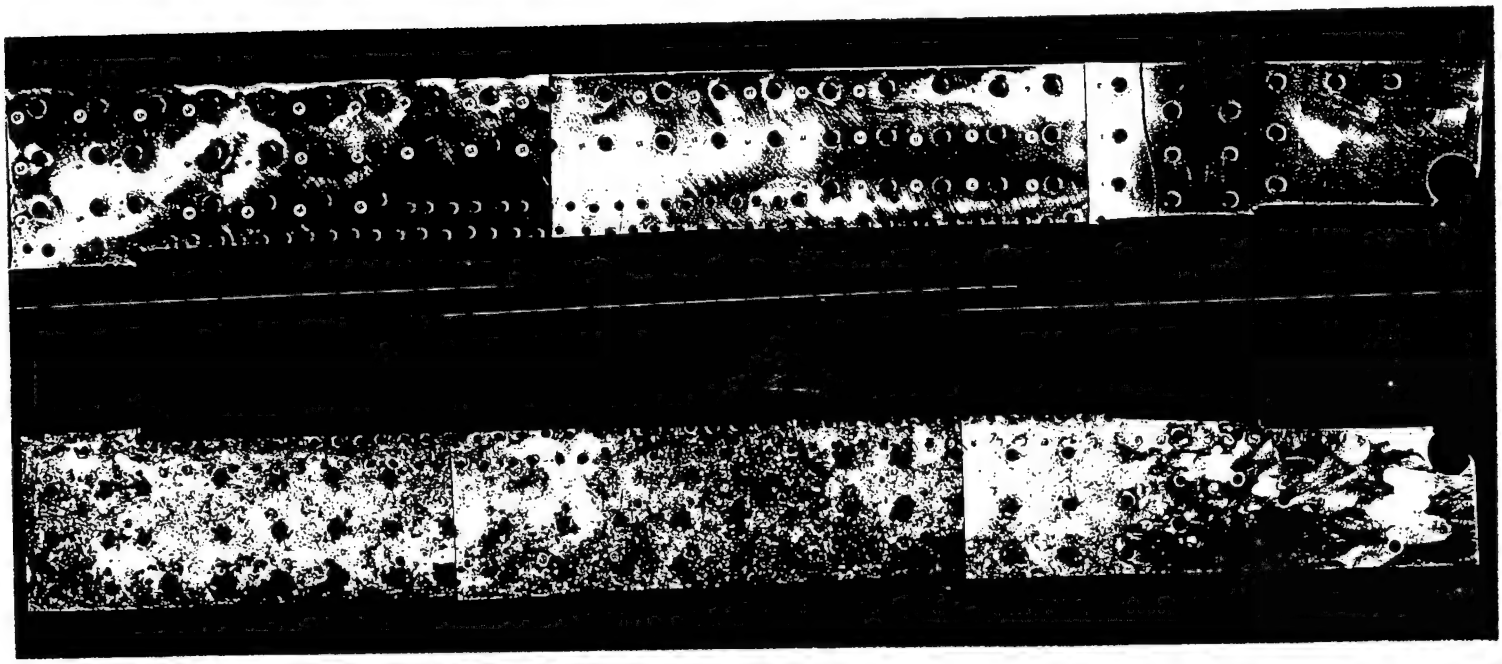

Figure 4.1. Faying Surface Of Lap Joint Section Of KC-135. (Top) Outside Surface (Bottom) Contact Or Faying Surface

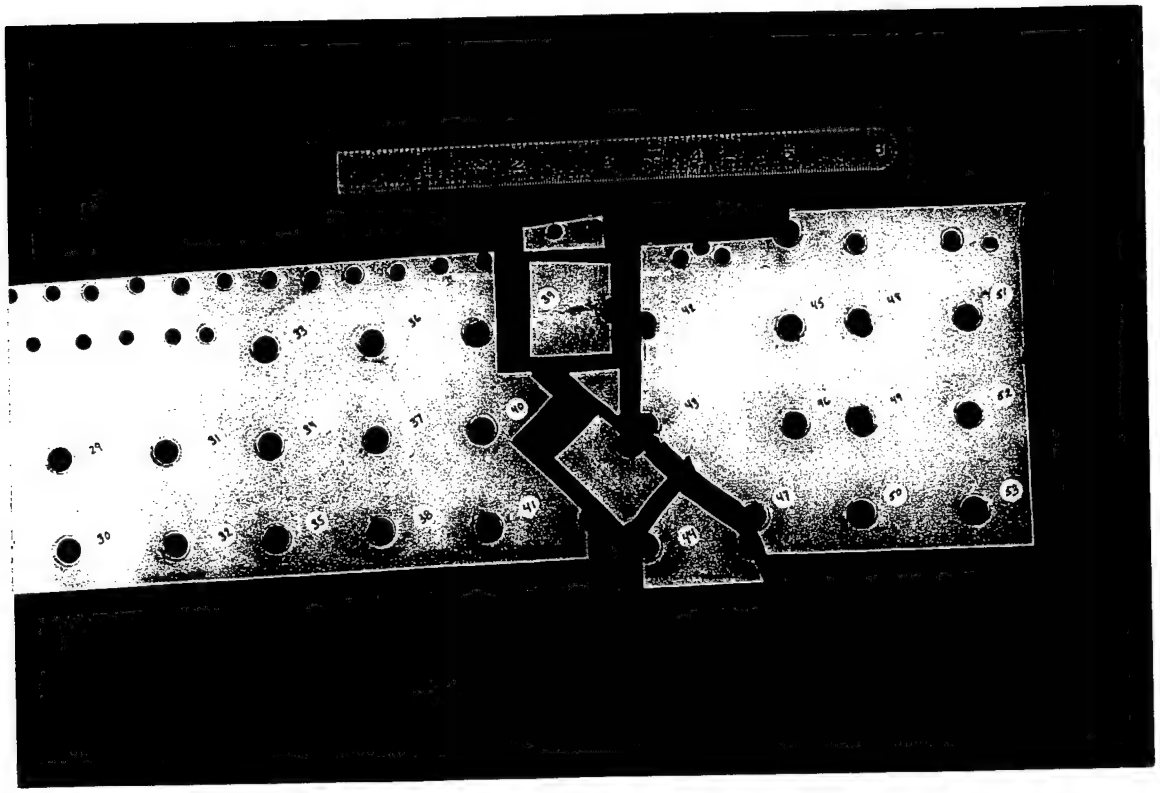

Figure 4.2. Outside Surface Of Lap Joint Sectionwith Cuts For Metallographic Cross Sectioning.

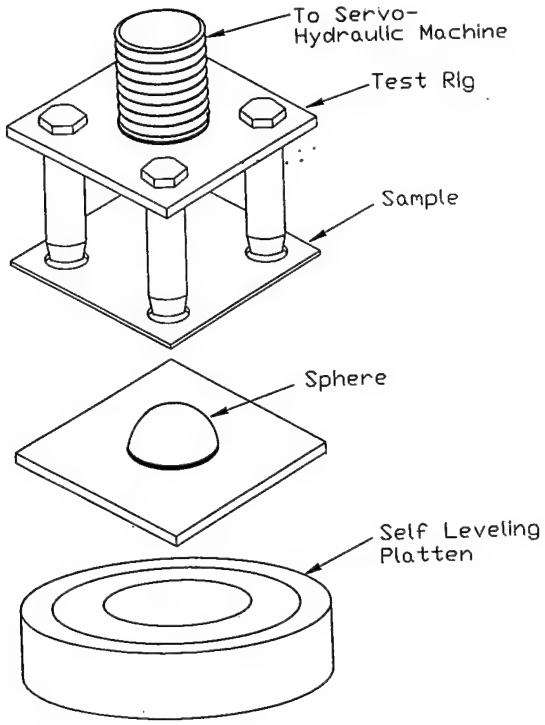

Figure 4.3. Schematic Drawing Of Test Rig To Simulate The Formation Of Corrosion By-Products In The Fuselage Lap Joint.

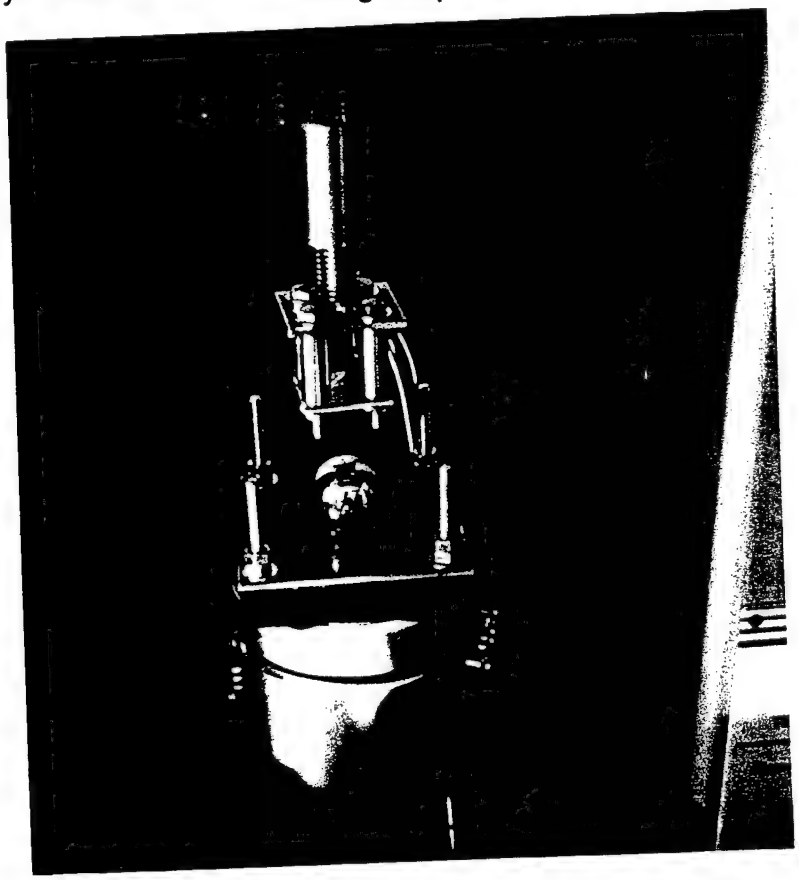

Figure 4.4. Test Rig In Servo-Hydraulic Machine.

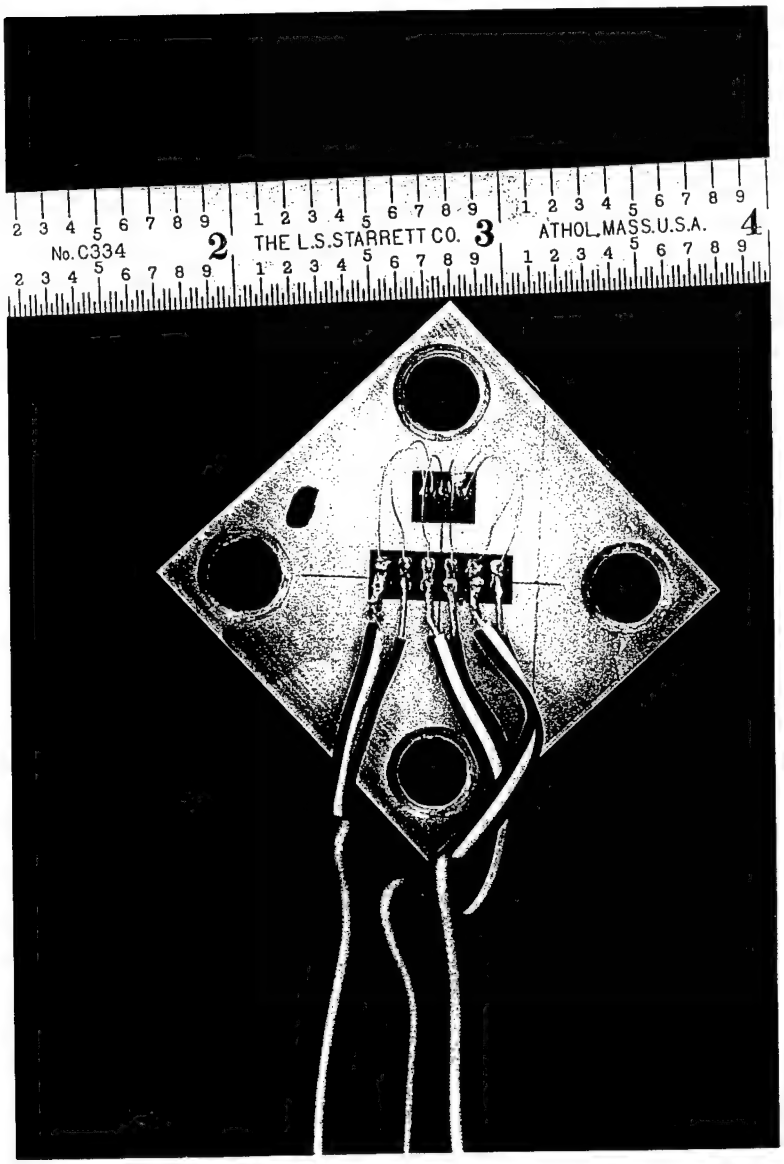

Figure 4.5. Test Coupon With Attached Strain Gage.

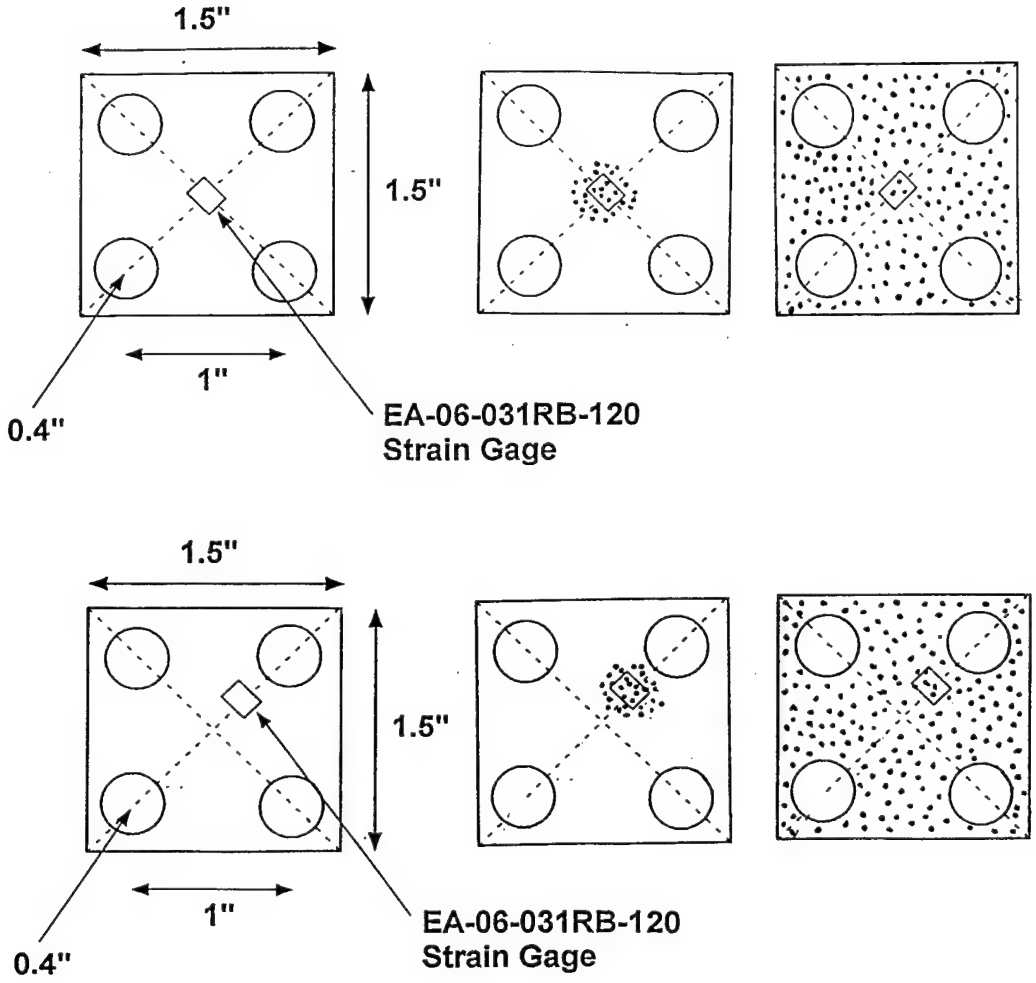

Figure 4.6. Schematic Drawing Of Coupons Indicating Corrosion Sites And Locations Of Strain Gages.

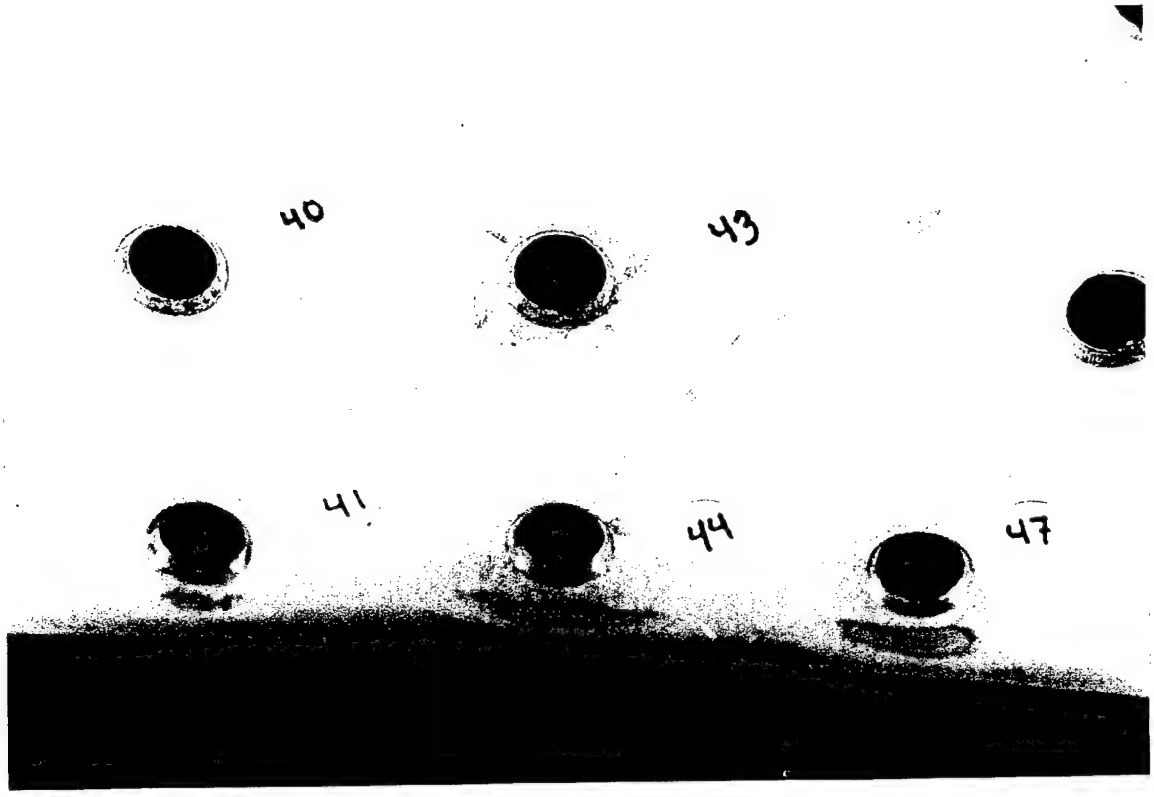

Figure 5.1. Outside Surface Of Lap Joint.

Figure 5.2. Close-Up Of Faying Surface Showing Extensive Corrosion.

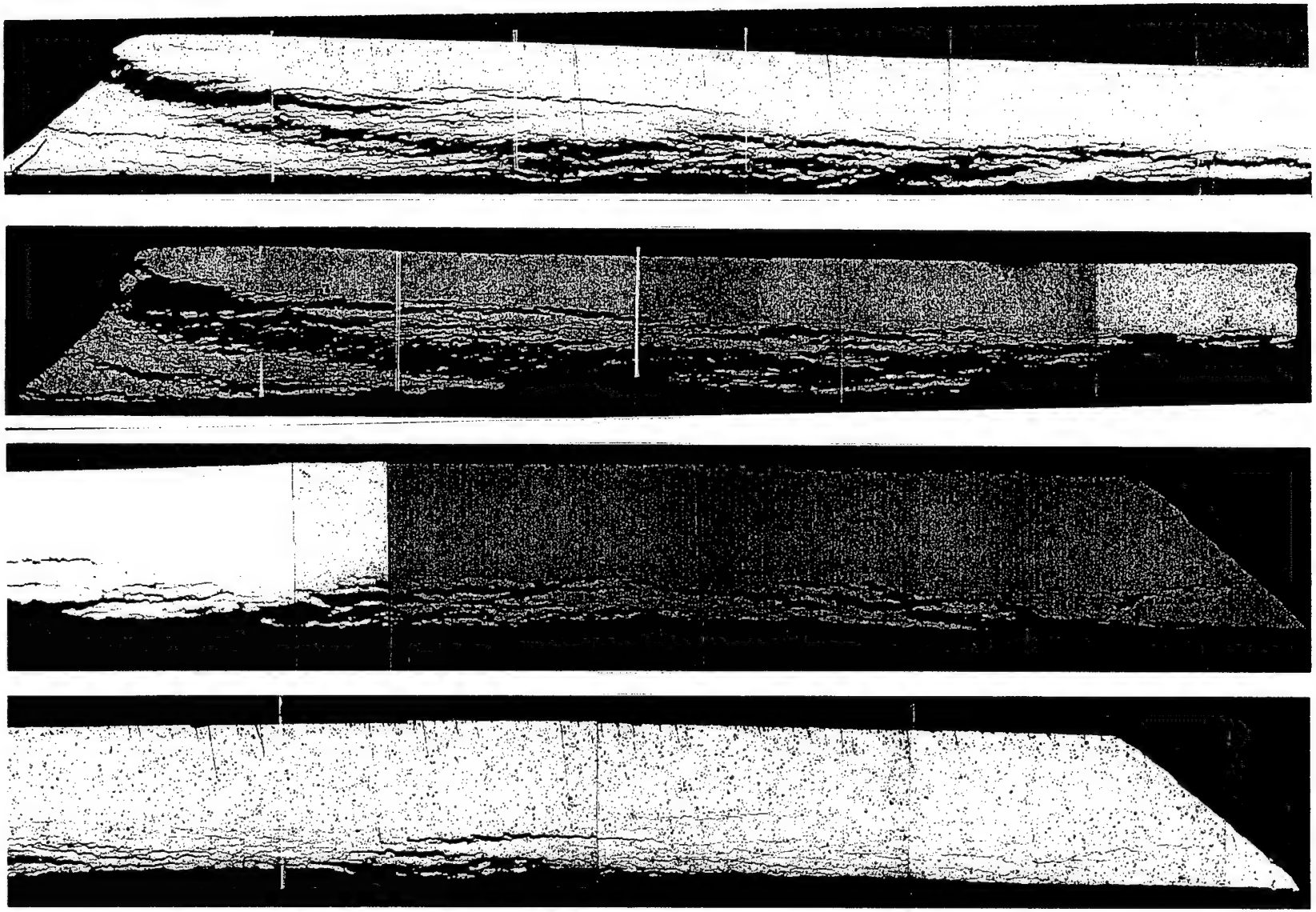

Figure 5.3. Metallographic Cross Sections Through Regions Adjacent To Fastener Holes.

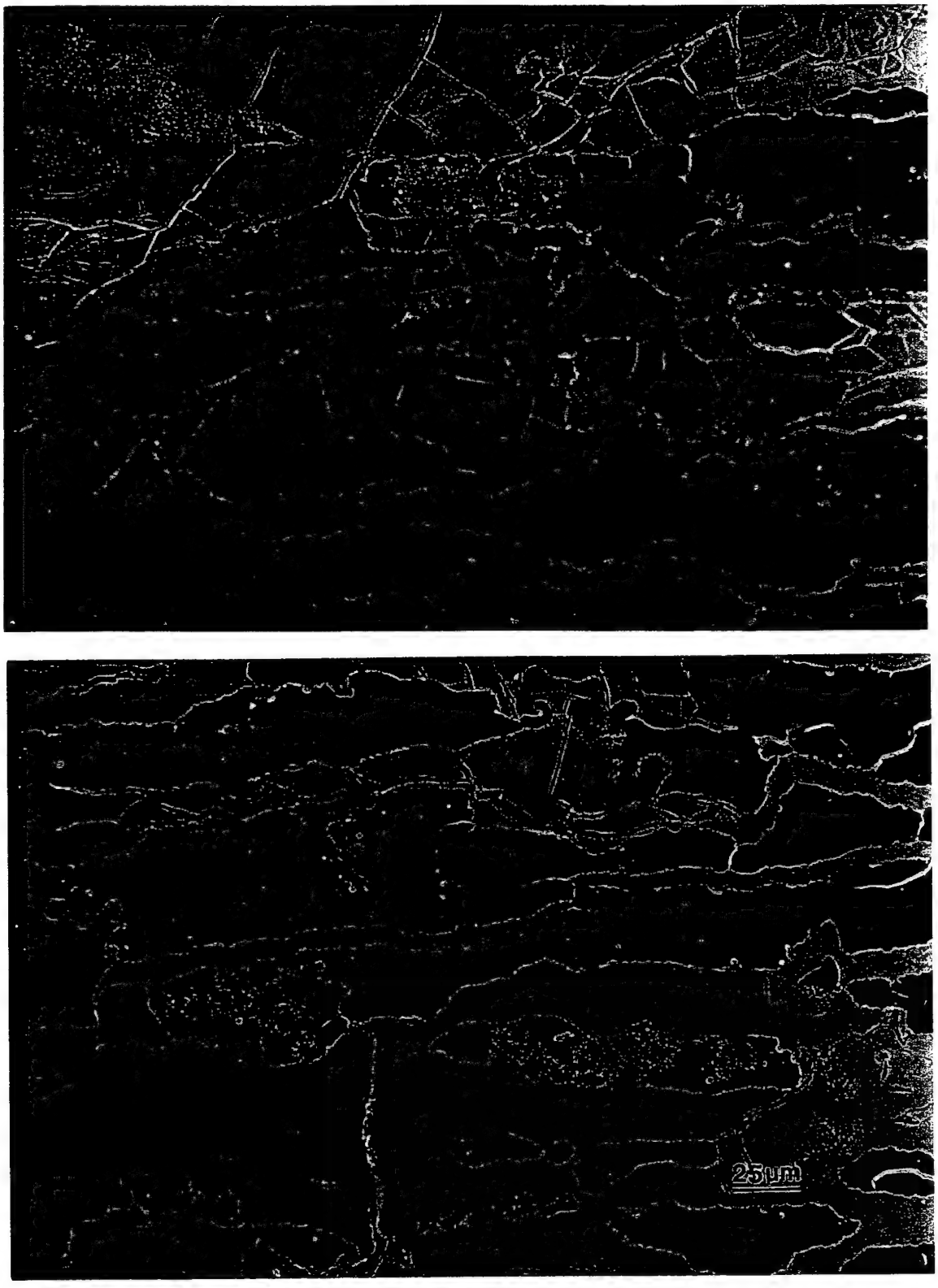

Figure 5.4. Optical Micrographs Of Exfoliated Grains Showing Preferential Dissolution Of A Phase Of The Aluminum Alloy.

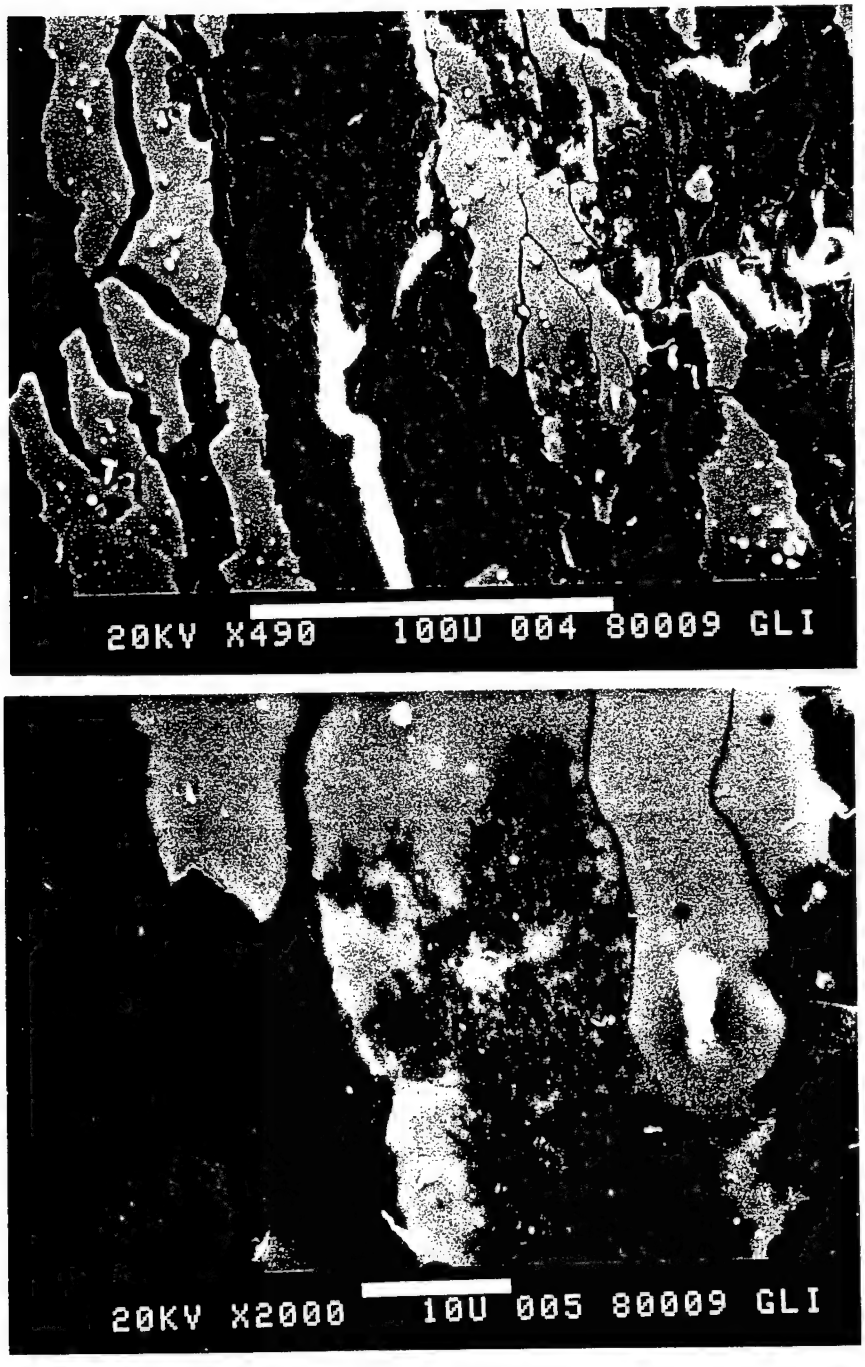

Figure 5.5. Scanning Electron Micrographs Of Exfoliated Grains.

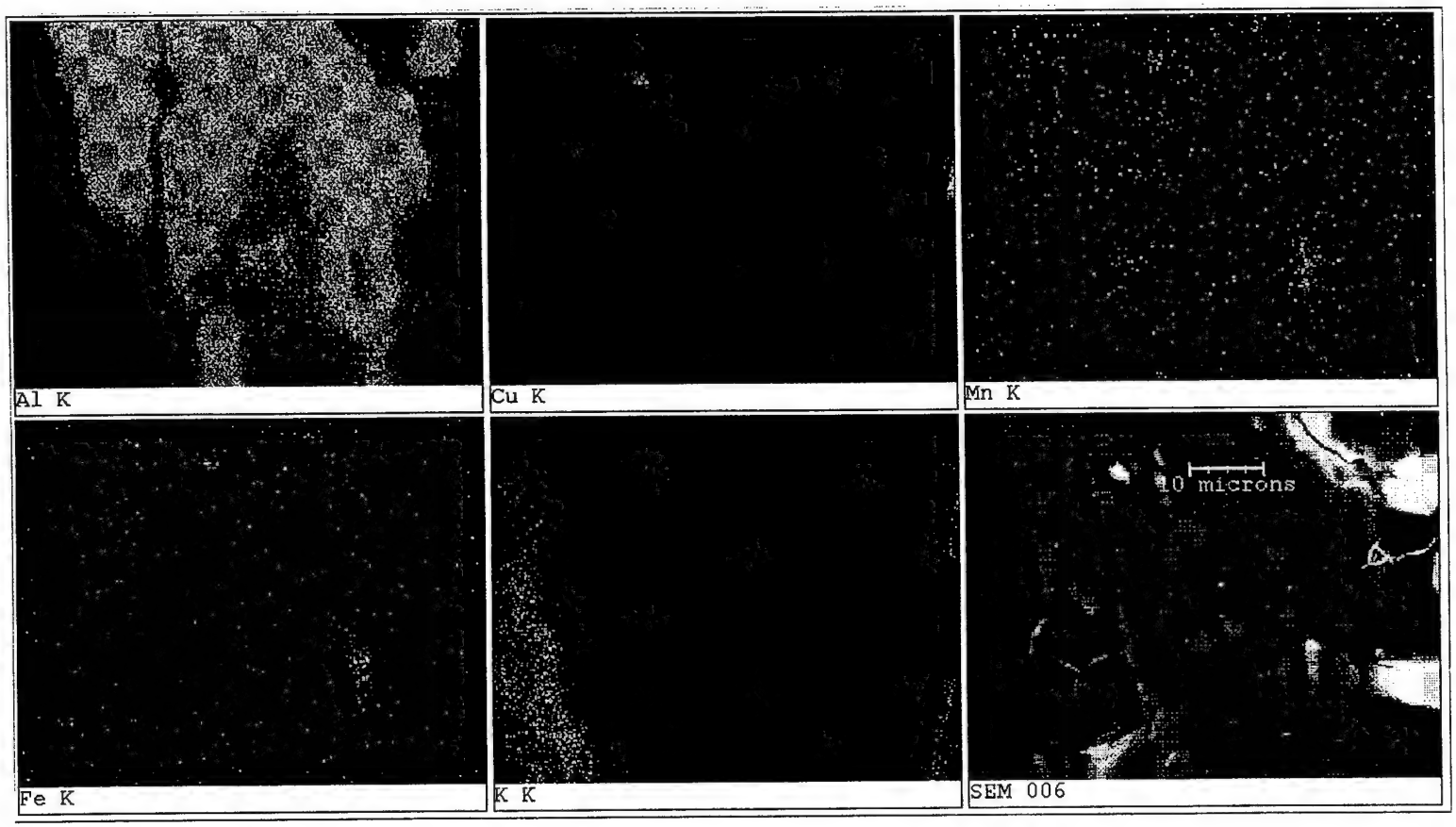

Figure 5.6. Electron Dispersive X-Ray Spectrographs Of An Exfoliated Grain, Showing Aluminum, Copper, Manganese, Iron, And Potassium Distribution.

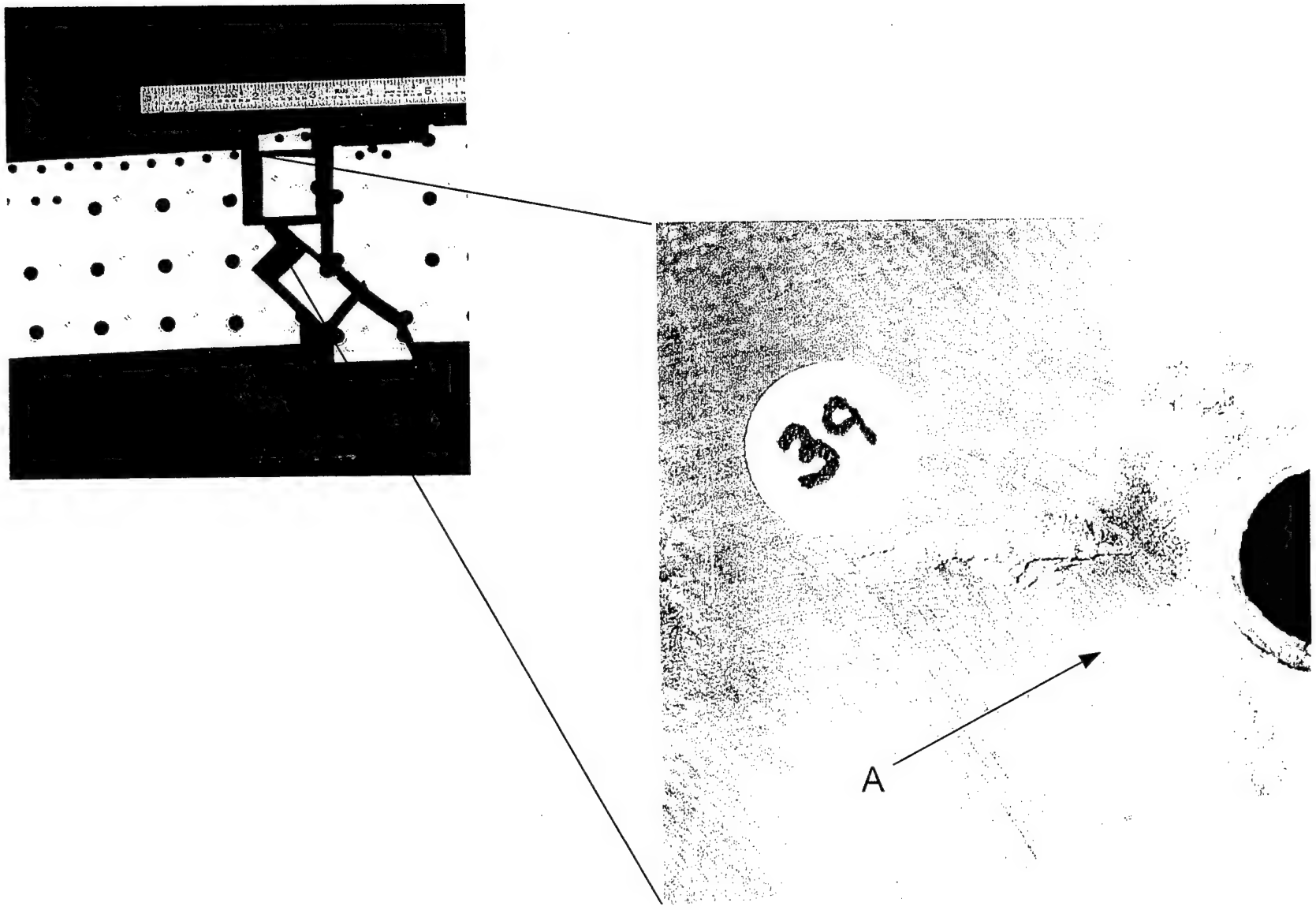

Figure 5.7 Detail Photograph of Area Adjacent to Fastener Hole 39.

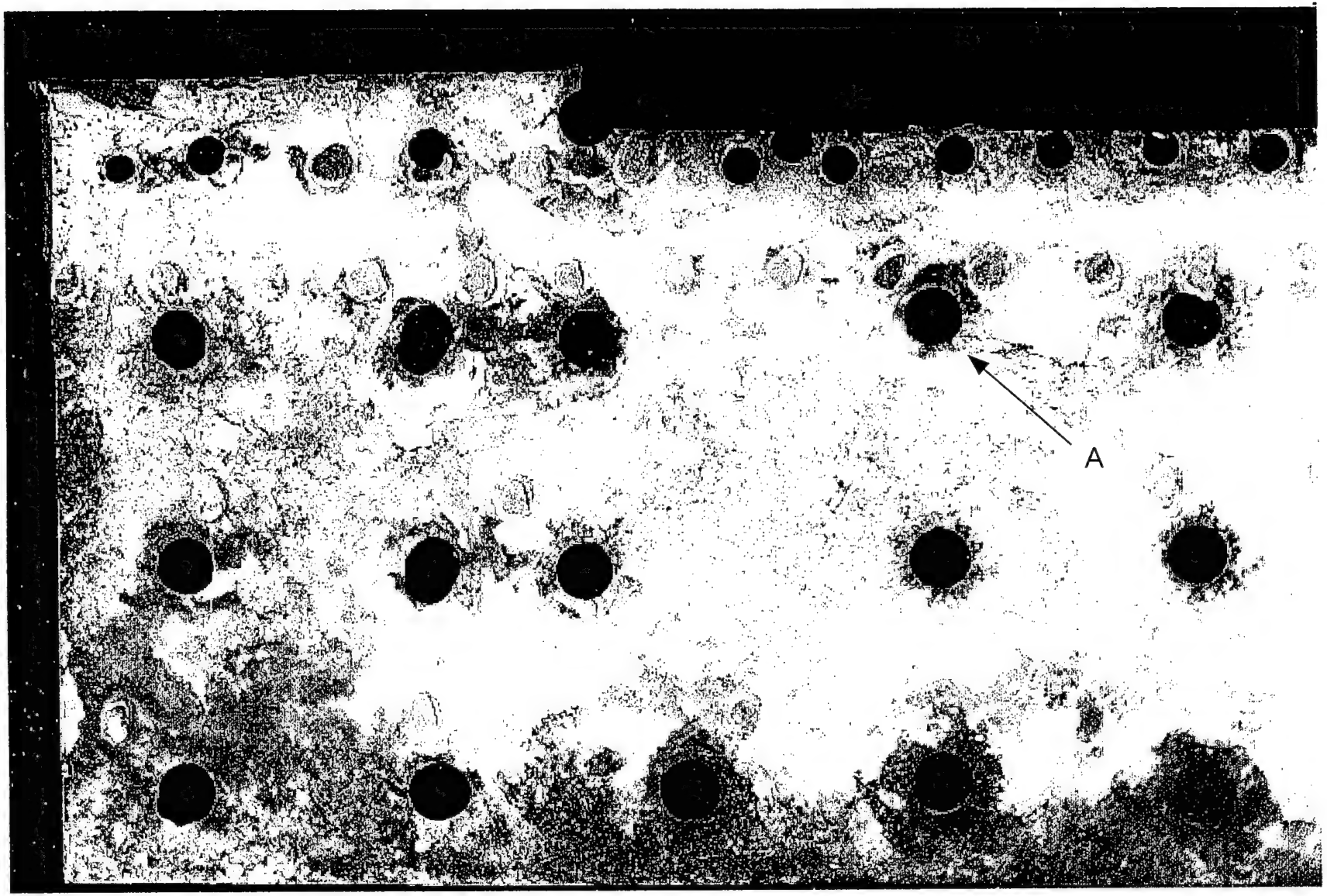

Figure 5.8 Faying Surface of the Lap Joint, Showing Area A Indicated in Figure 5.7.

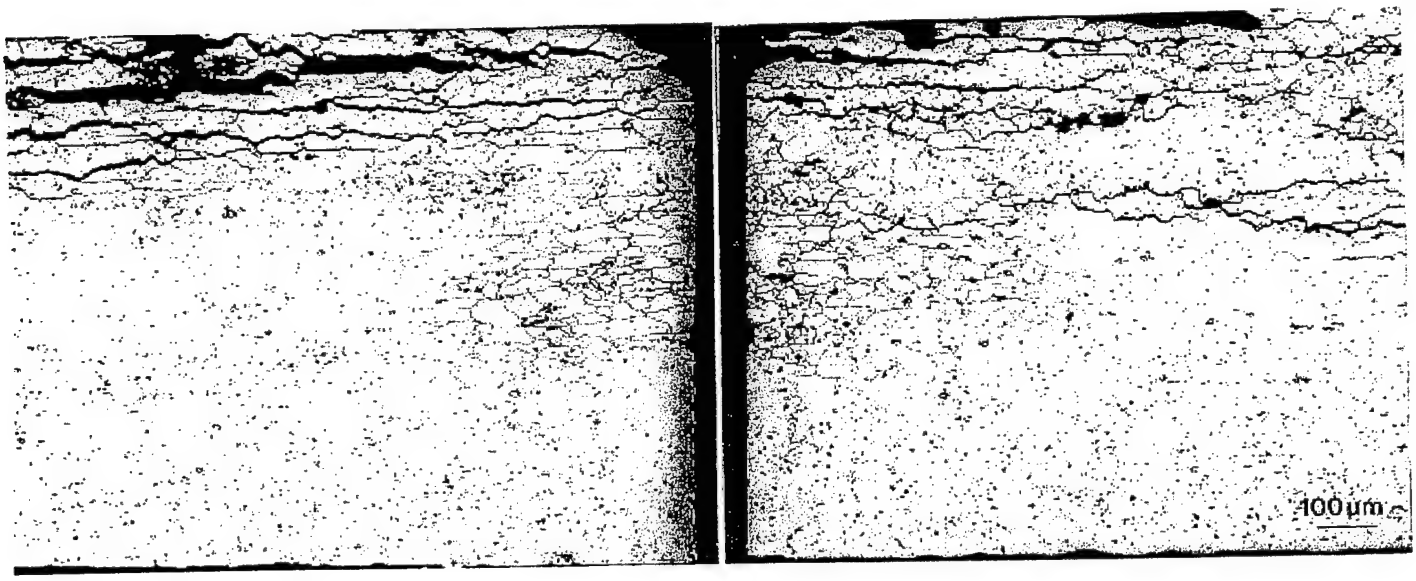

Figure 5.9. Matching Optical Micrographs Of Cross Sections Through Area A In Longitudinal And Transverse Direction.

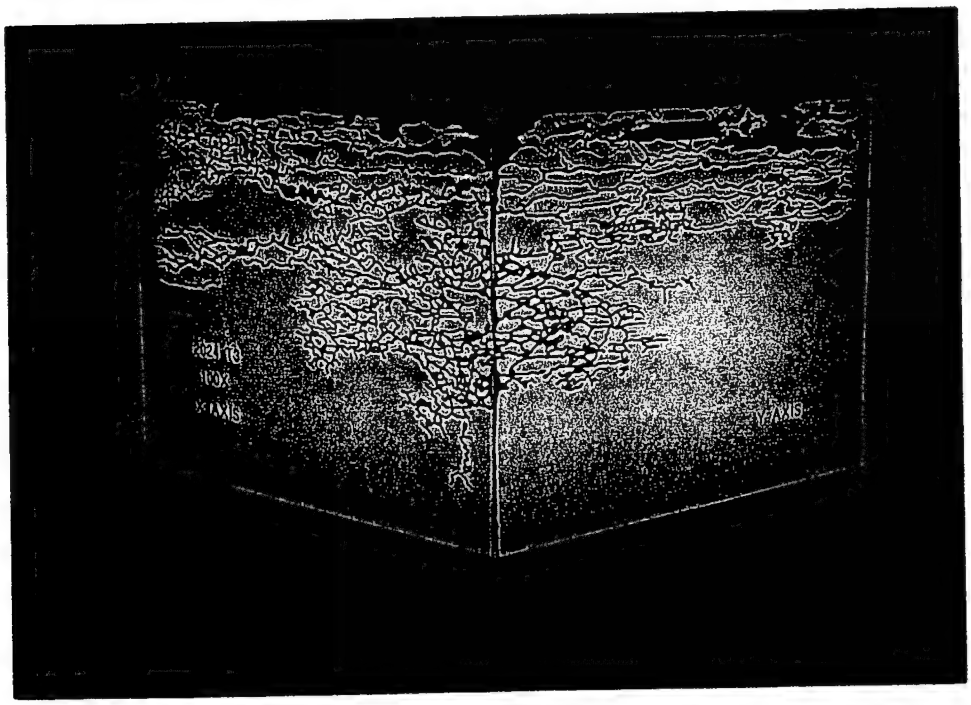

Figure 5.10. Three-Dimensional Image Of Optical Micrographs Showing In Figure 5.9.

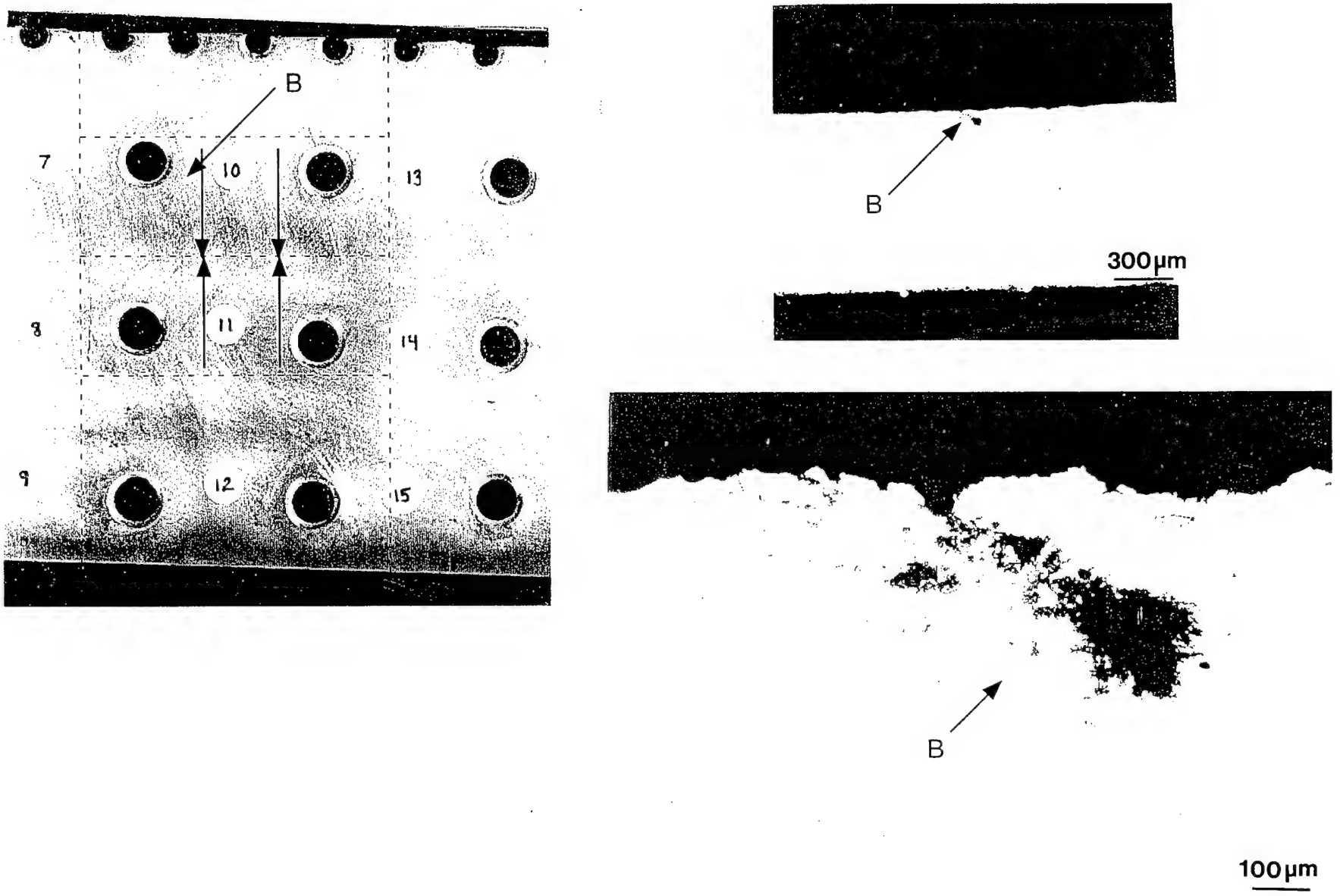

Figure 5.11 Composite Figure Showing Outside Surface of Lap Joint, which Indicates Area B where a Longitudinal Cross Section Was Made. A B a Pit and Intergranular Corrosion can be Seen.

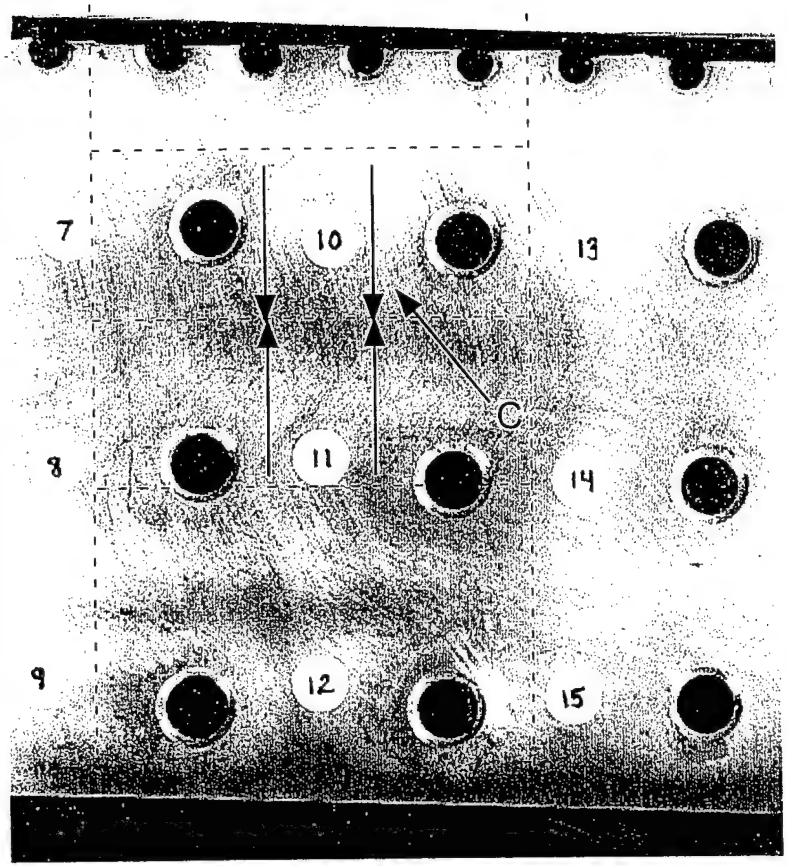

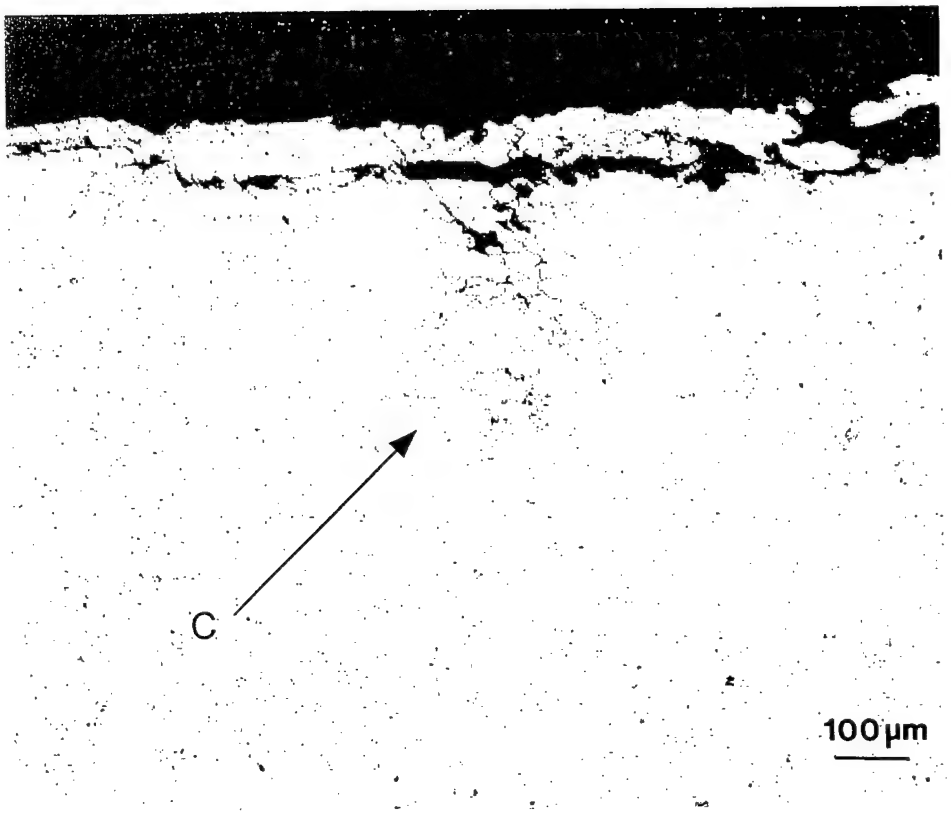

Figure 5.12 Composite Figure Showing Outside Surface of Lap Joint, which Indicates Area C where a Longitudinal Cross Section was Made. Exfoliation Corrosion and Deep Intergranular Corrosion can be Seen.

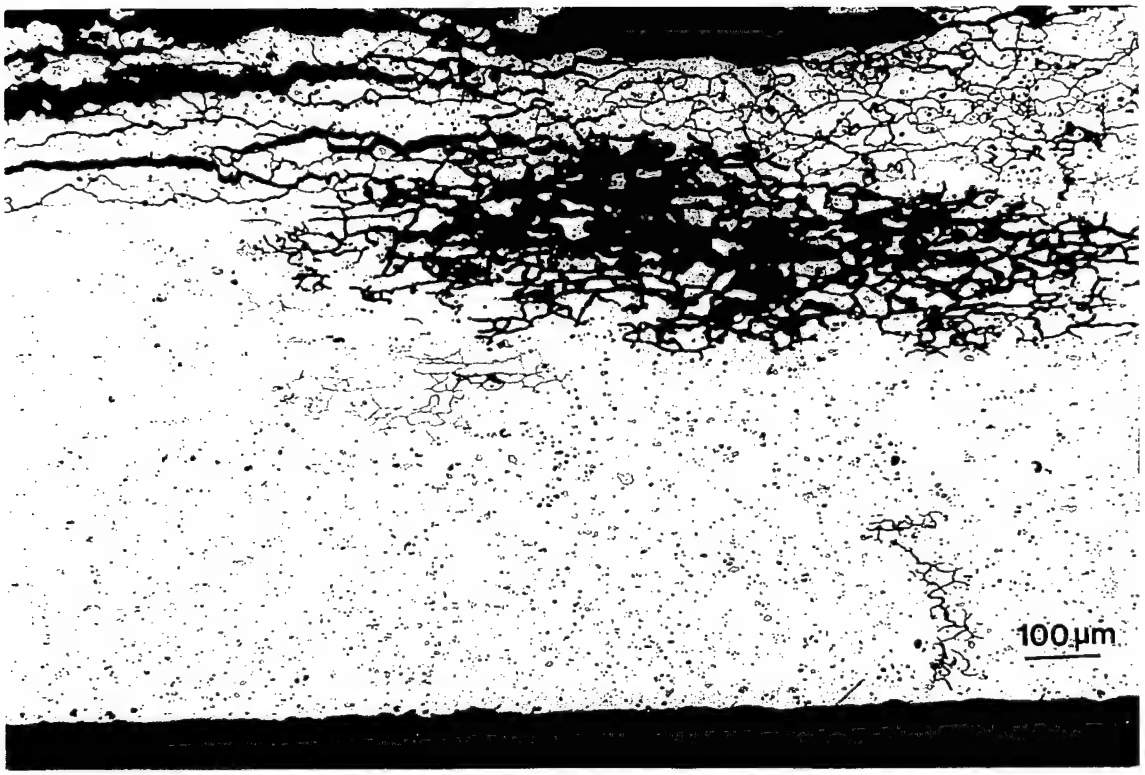

Figure 5.13. Optical Micrograph Of Metallographic Cross Section Through Lap Joint Section Showing Increased Attack Of The Grain Boundaries.

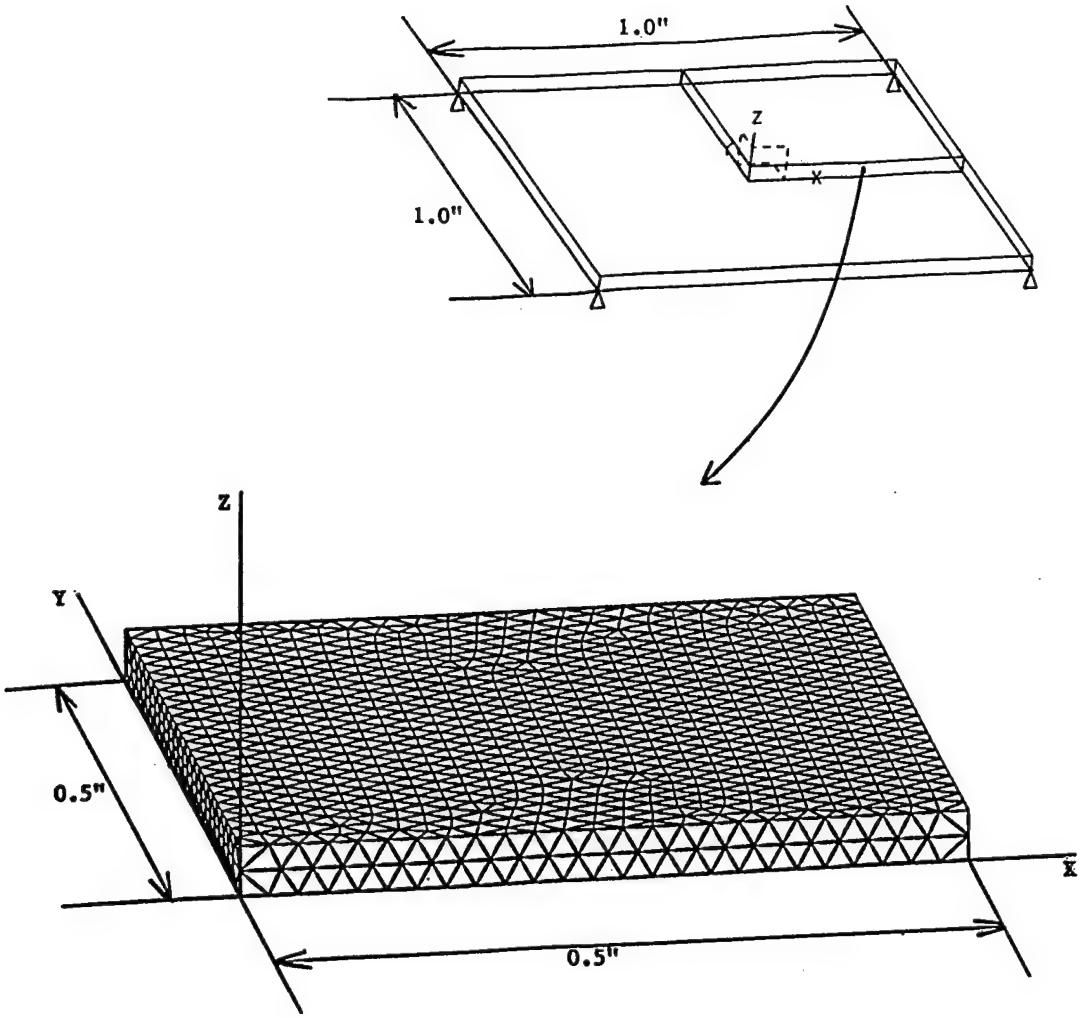

Figure 5.14. Finite Element Mesh For Quarter Of Plate With Pin Connections In The Corner.

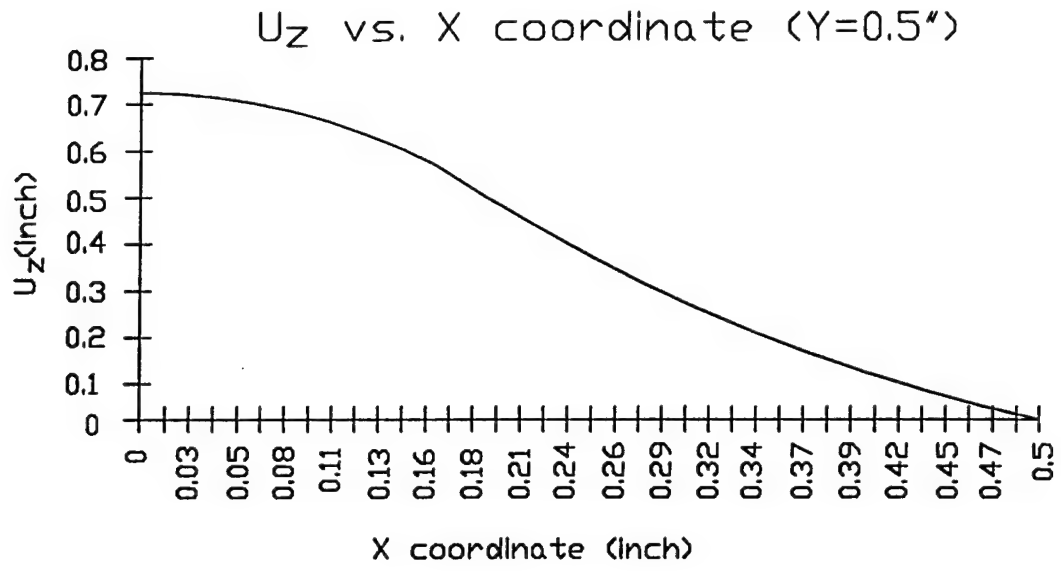

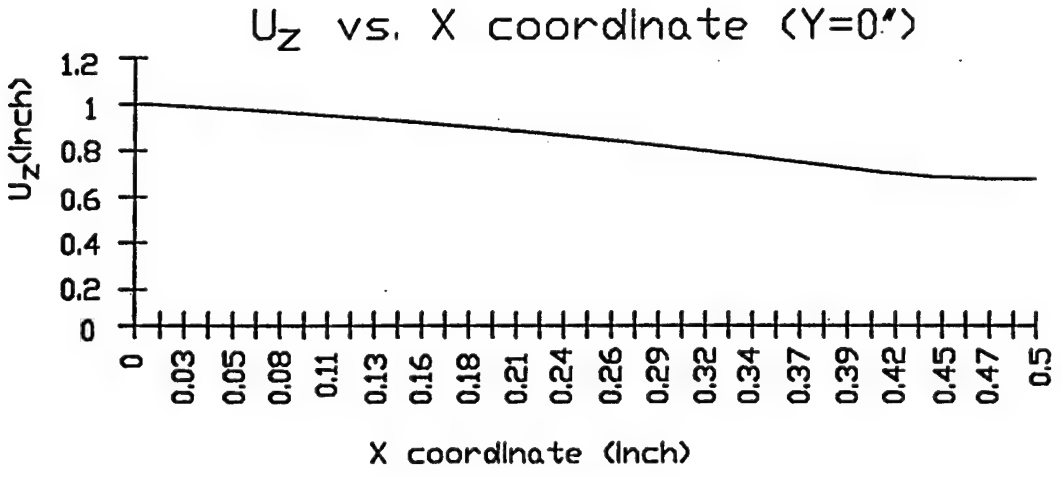

Figure 5.15. Diagrams Of Displacement In The Z-Direction U_z As A Function Of X And Y Coordinates In Figure 5.14. The Curves Showing In The Figure Are Calculated With ABAQUS And Match The Theoretical Curves By Timoshenko For A Plate Thickness Of 0.018 Inch.

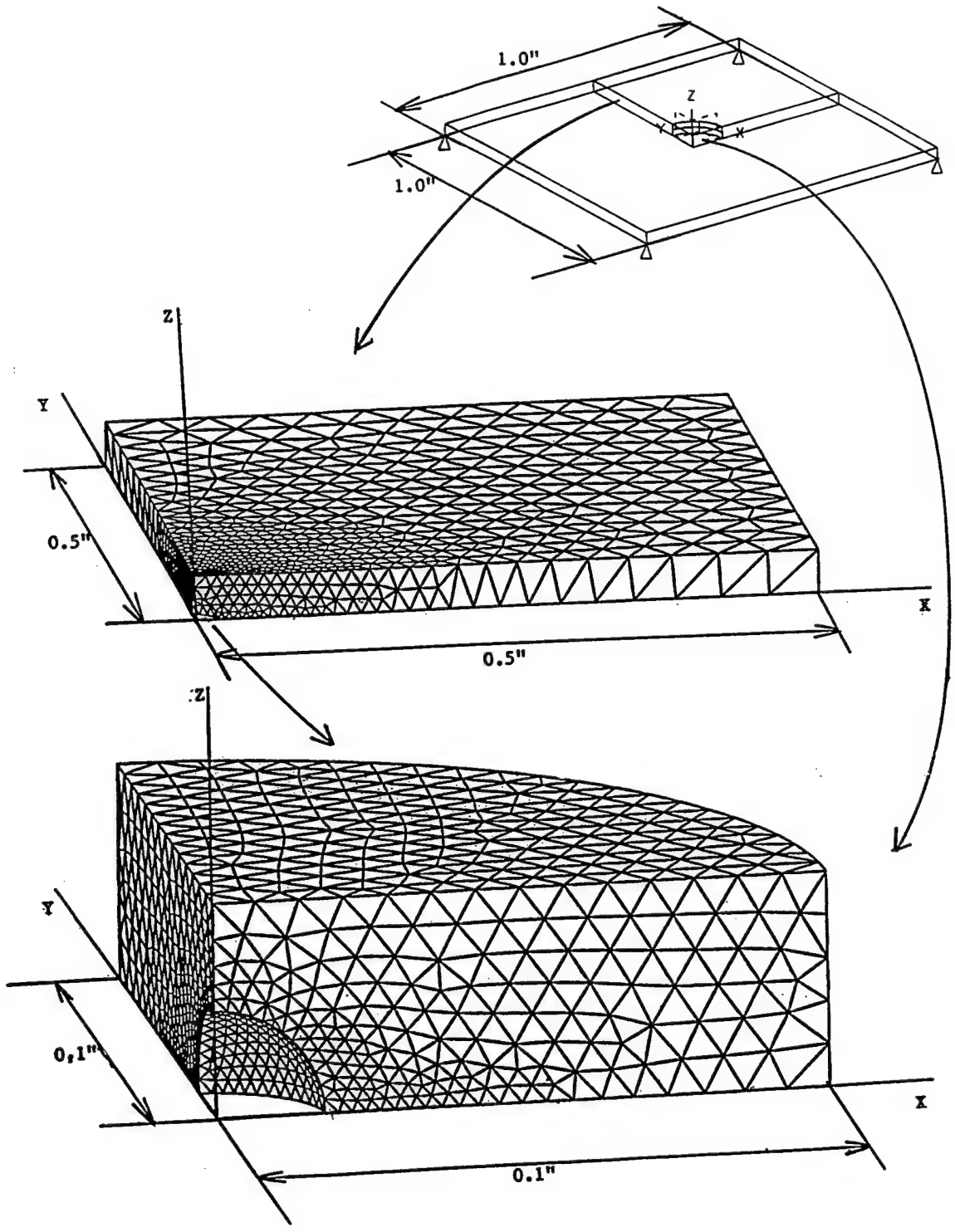

Figure 5.16. Macro-Micro Finite Element Mesh For A Hemispherical Indent In The Middle Of The Plate.

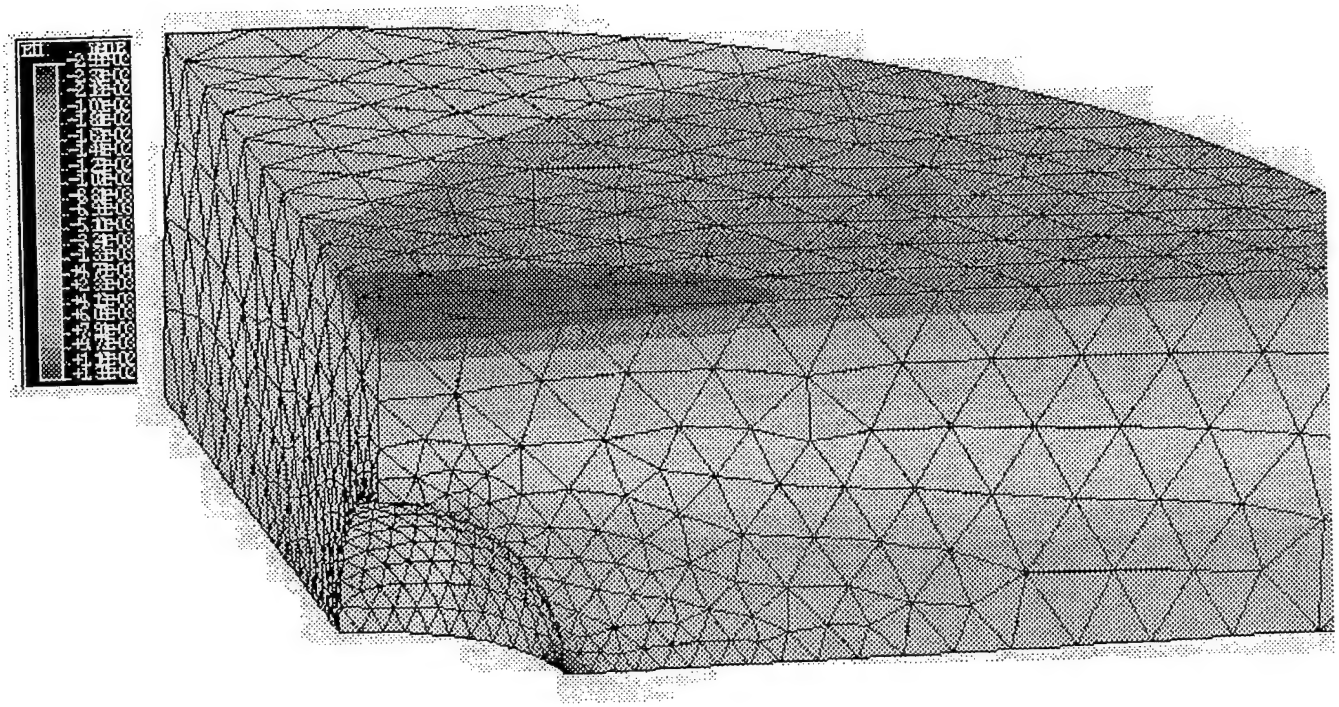

Figure 5.17. Normal Strain Distribution In The Diagonal Direction Of Region Near The Hemispherical Indent.

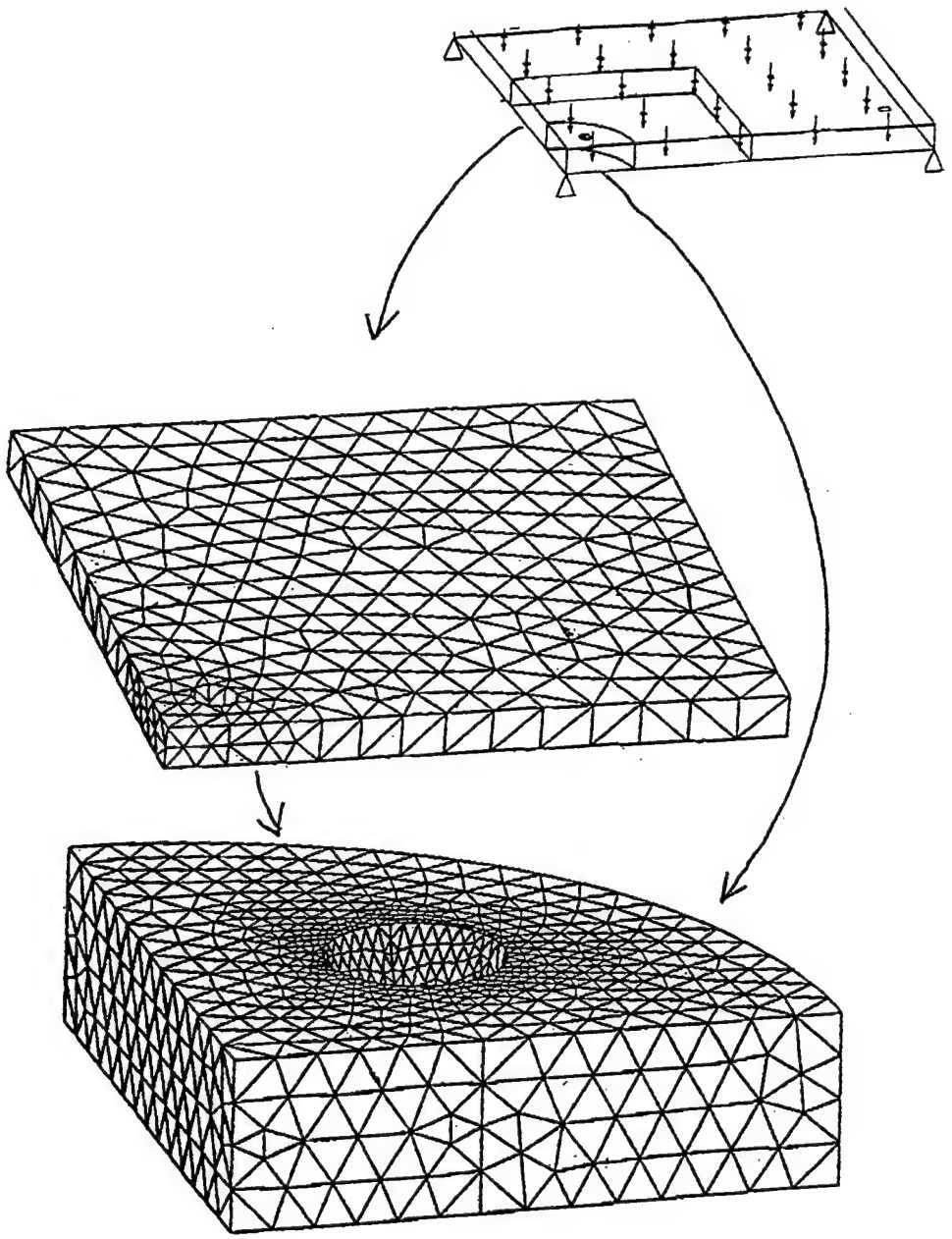

Figure 5.18. Finite Element Mesh For Tetrahedron Elements Showing One Quarter Of The Loaded Sheet With A Hemispherical Indent Close To The Pin Connection. The Mesh Is For An Area Around The Hemisphere With A Radius Of 0.1 Inch.

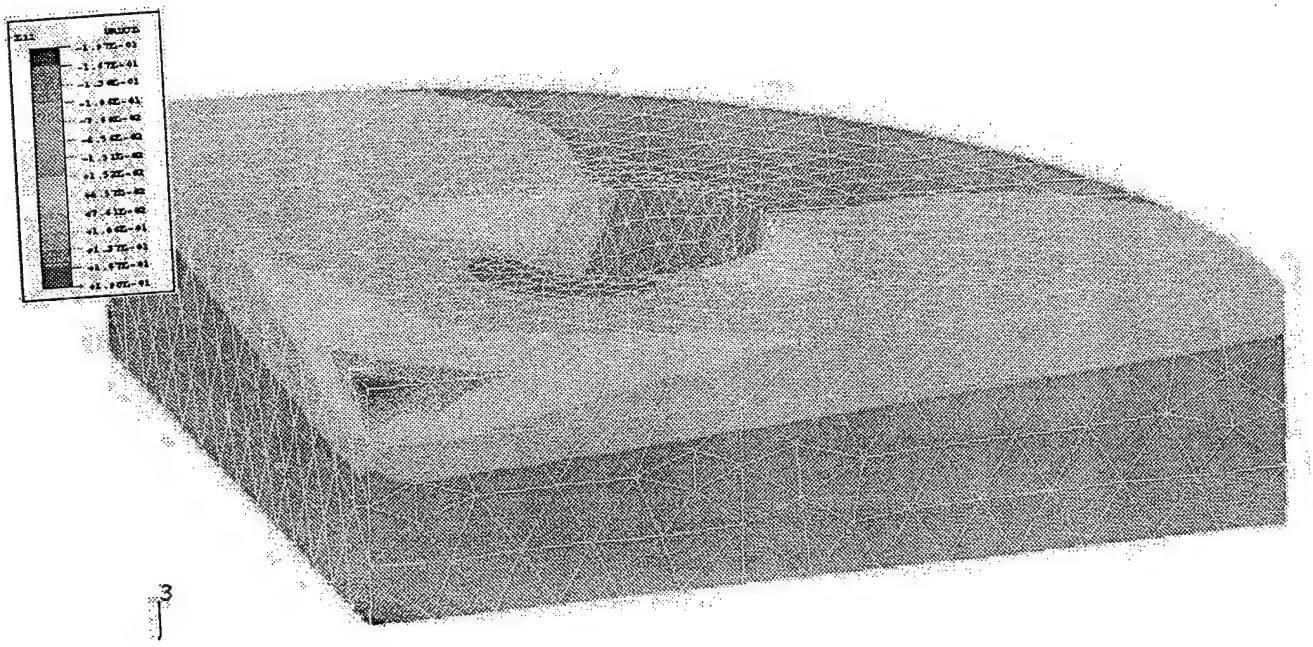

Figure 5.19. Normal Strain Distribution (In Diagonal Direction) In The 0.1 Inch Radius Region. The Maximum Strain Level Is 0.07 Around The Hemisphere. The Maximum Strain Level In The Same Location Without The Hemisphere Is 0.037.

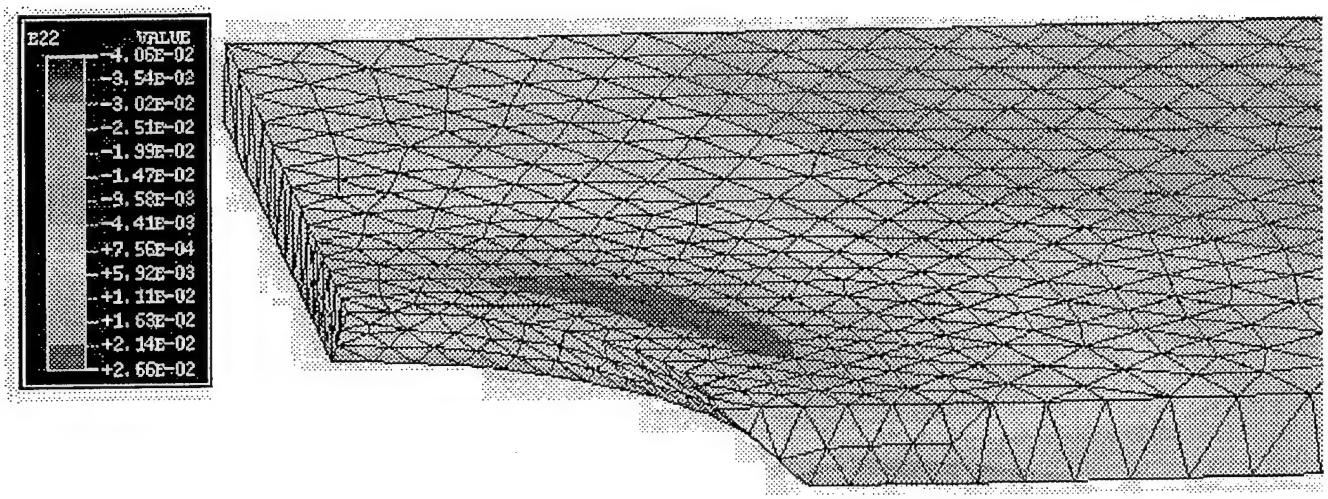

Figure 5.20. Normal Strain Distribution (In Diagonal Direction) In The Quarter Of The Loaded Sheet With A Realistic Geometry Of The Fastener Hole. Displacement Zero Conditions On The Fastener Hole And Pressure Are Applied In The Vertical Direction.

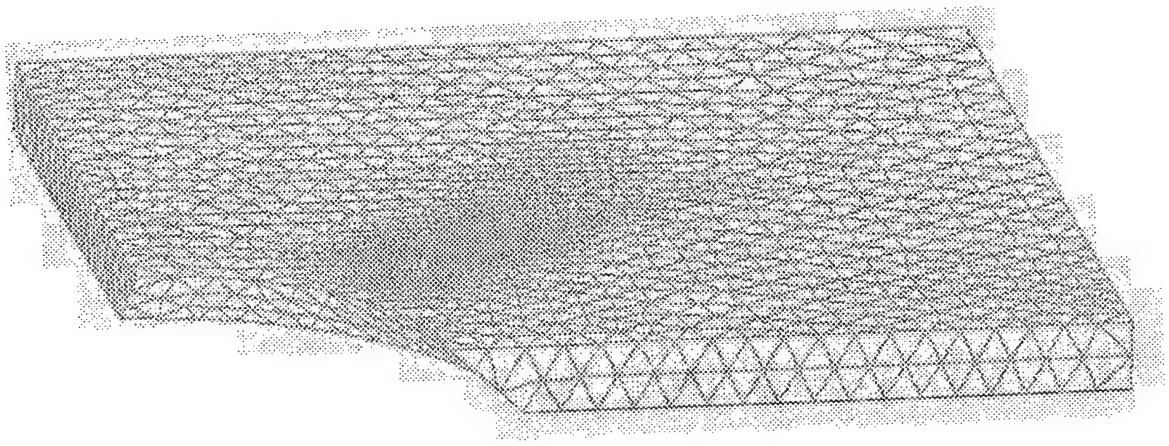

Figure 5.21. FEM Mesh Of Quarter Sheet With Realistic Fastener Hole And Hemisphere With Radius Of 0.018 Inch Located 0.198 Inch From The Center Of The Fastener Hole.

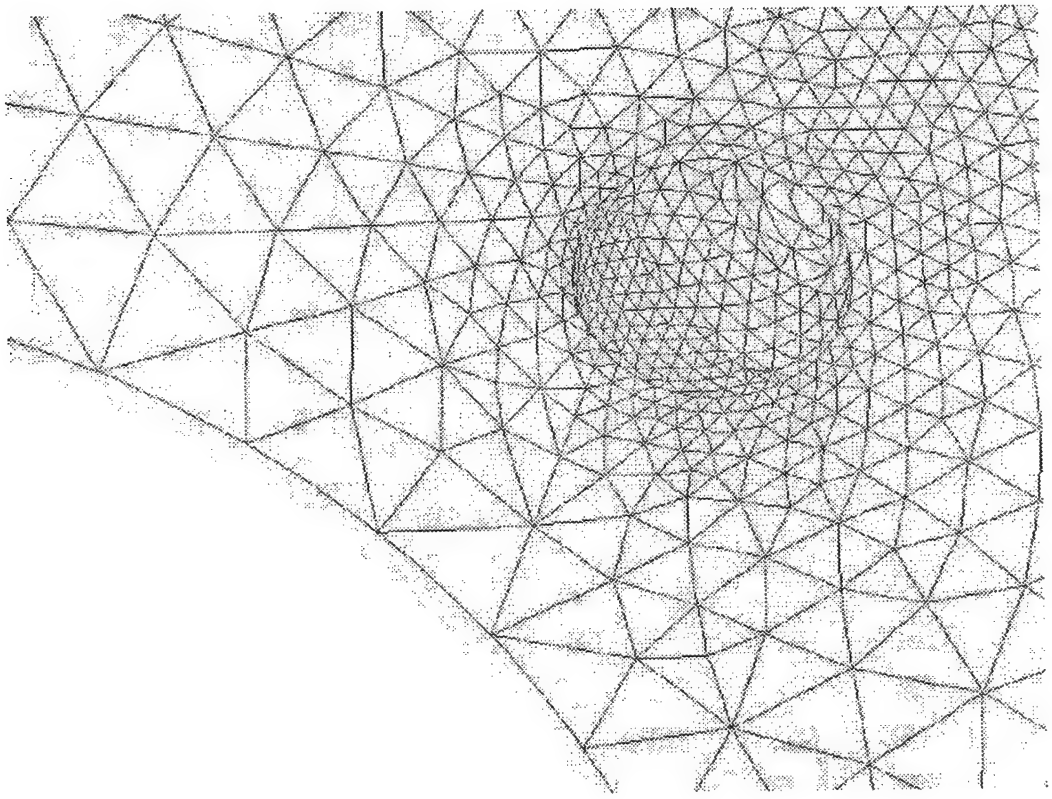

Figure 5.22. Local View Of T Fine Mesh Around The Hemisphere Showing In Figure 5.21.

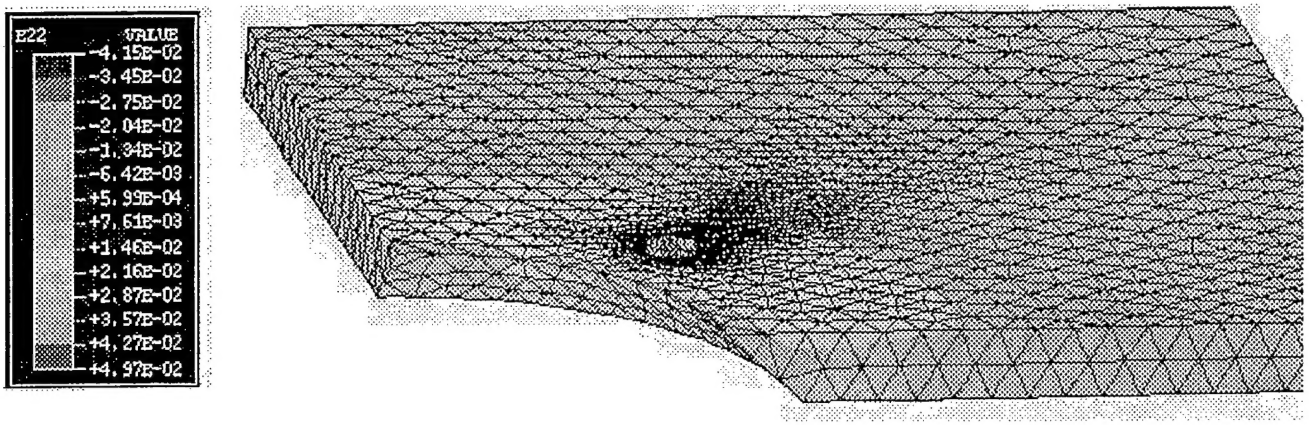

Figure 5.23. Normal Strain In The Diagonal Direction Of Plate Shown In Figures 5.21 And 5.22.

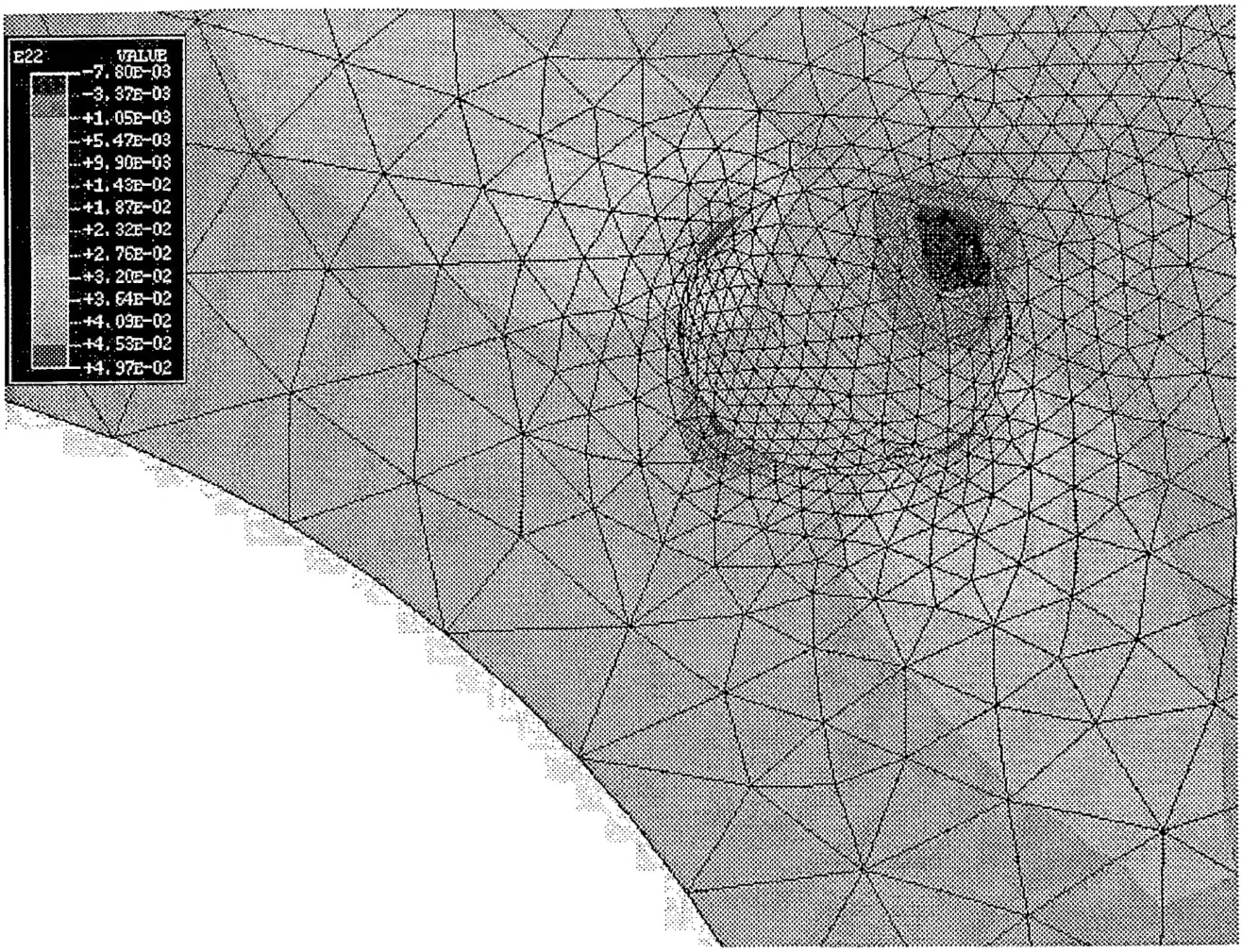

Figure 5.24. Local View Of Normal Strain In The Diagonal Direction Around The Hemisphere.

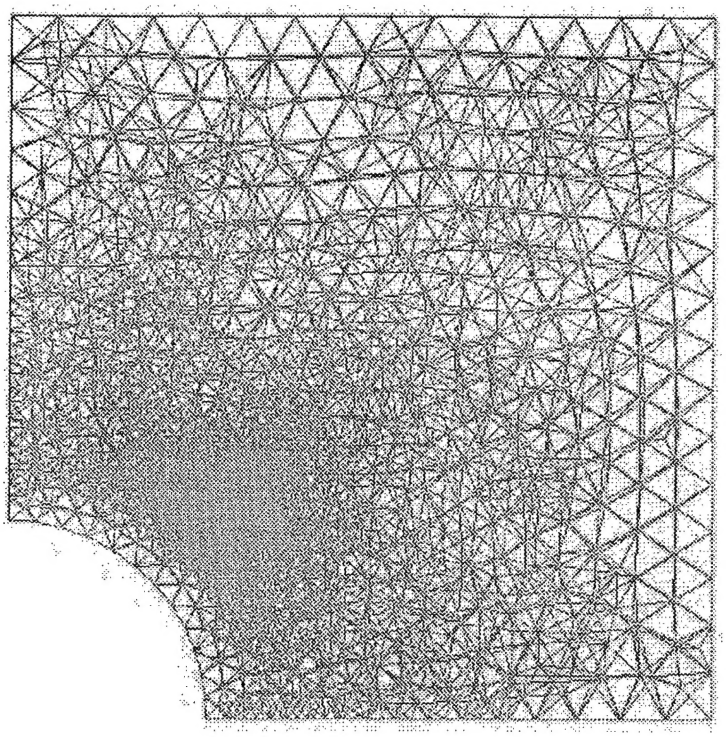

Figure 5.25. Finite Element Mesh With 0.009 Inch Radius Hemisphere Located At 0.198 Inch From The Center Of The Fastener Hole (18998 10-Node Tetrahedron Elements)

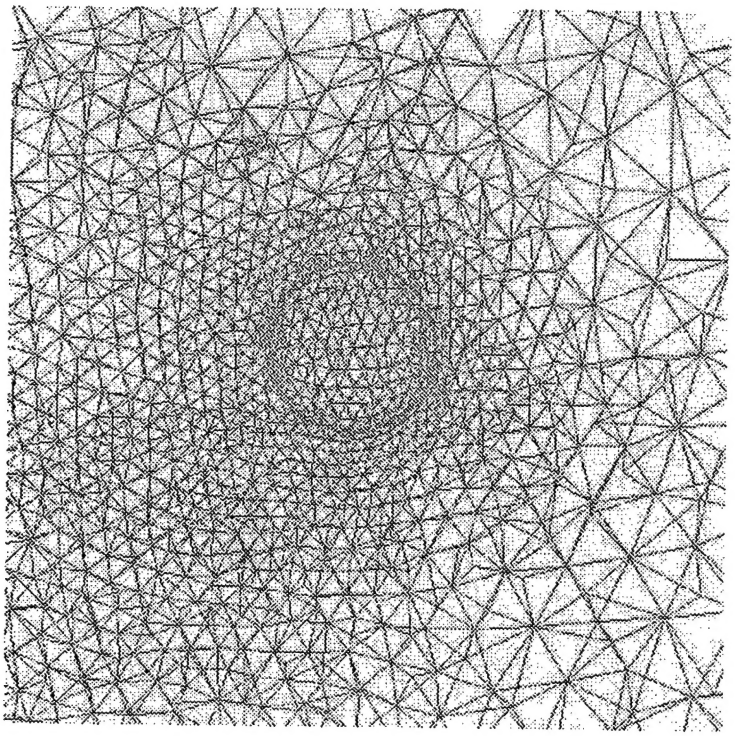

Figure 5.26. Local View Of The Fine Mesh Around The Hemisphere.

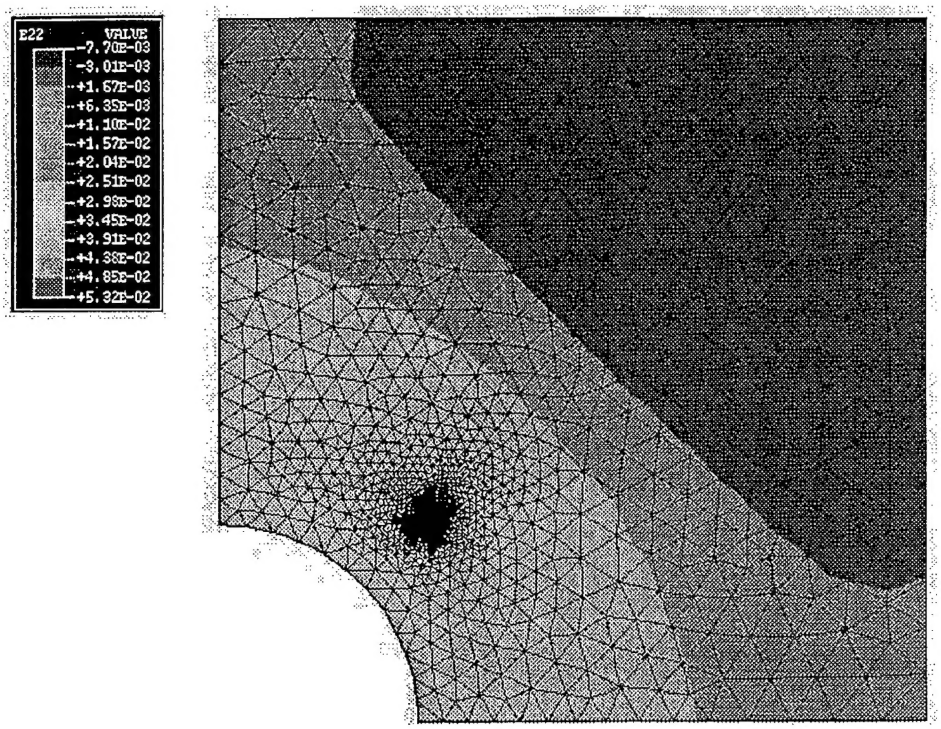

Figure 5.27. Normal Strain In The Diagonal Direction Of Plate Shown In Figures 5.24 And 5.25.

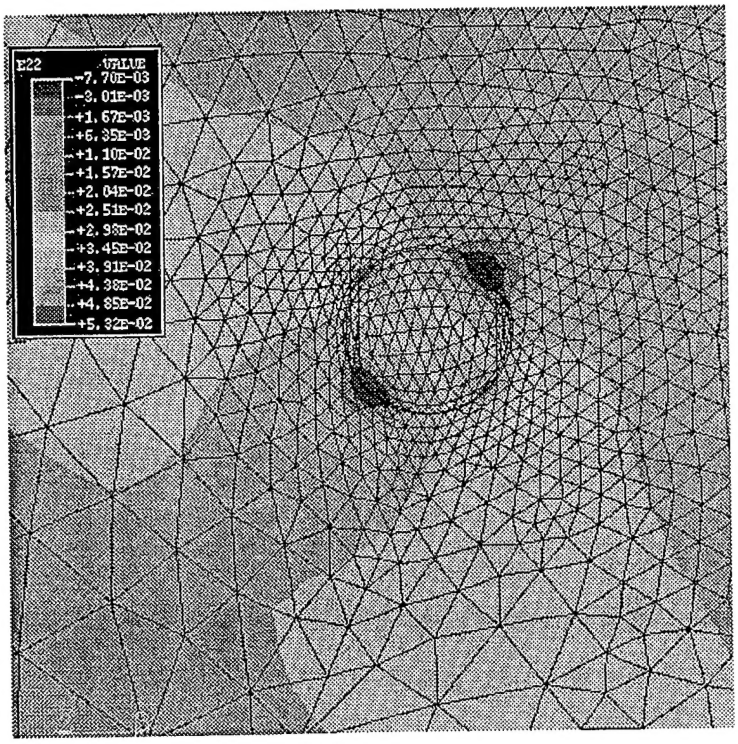

Figure 5.28. Local View Of The Normal Strain The Diagonal Direction Of Figure 5.27.

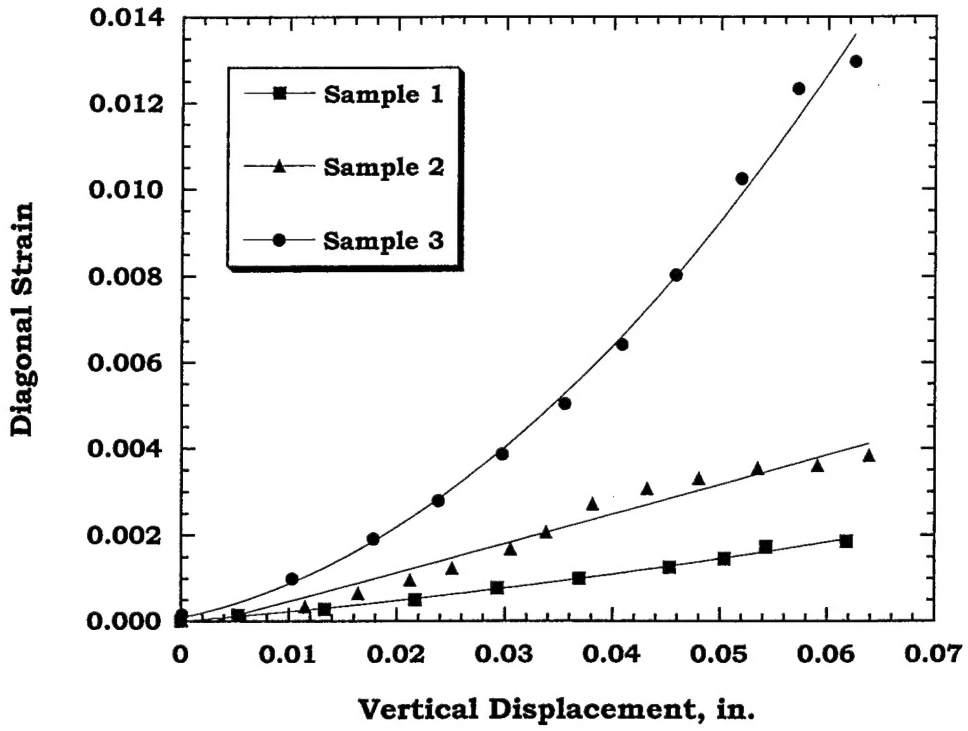

Figure 5.29. Local Strain At The Center Of Plate In Diagonal Direction As A Function Of Vertical Displacement. 1) Plate Without Corrosion; 2) Plate With Uniform Corrosion; 3) Plate With Localized Corrosion In Center.